patients who were treated with bisphosphonate. Although no clinical symptoms owing to hypocalcemia were noted, five of 11 patients treated with bisphosphonate and none of those treated without bisphosphonate required calcium supplementation. During the therapies for hypercalcemia, precipitation of calcium phosphate in urine was noticed in Cases 9, 10 and 14, and renal calculus developed in Case 10.

Treatment outcome of leukemia

All patients achieved complete remission (CR), but leukemia relapsed in 11 patients including Case 14 who developed AML at relapse (Table 1). The EFS rate at 5 years from diagnosis of ALL was estimated as 46.2±11.7%. Of note, all five patients with t(17;19)-ALL relapsed very early and their 5-year EFS rate (0%) was significantly lower ($p<0.0001$ in log-rank test) than that of the other 17 patients (59.7±13.4%). Among the 18 patients who developed hypercalcemia at disease onset (excluding Cases 1, 2, 5 and 7), the 5-year EFS rate of two patients with t(17;19)-ALL (0%) was still significantly lower ($P<0.0001$ in log-rank test) than that of the other 16 patients (63.5±13.7%). Thus, excluding the patients with t(17;19)-ALL, the 5-year EFS rate of ALL patients accompanied by hypercalcemia is almost similar to that of childhood ALL patients in the TCCSG treated with L89-12, L92-13,[25] L95-14 (1995–1999; 596 patients), and L99-15 (1999–2003; 623 patients) protocols, in which the 5-year EFS rate was 67.8±2.3, 63.4±2.7, 76.0±1.9 and 76.4±2.5%, respectively.

Discussion

This is the first cohort study of hypercalcemia associated with childhood ALL, and we retrospectively analyzed 22 Japanese patients reported in the last 15 years. Despite several limitations in a retrospective study, the present study newly demonstrated some characteristics of childhood ALL accompanied by hypercalcemia. The incidence of onset at age 10 years and older among the patients with hypercalcemia in the present study was significantly higher than that among all childhood ALL patients. Most of our patients had a low initial WBC and two-thirds of our patients had mild anemia and normal to mildly low platelet count, suggesting that symptoms associated with hypercalcemia rather than hematological abnormalities might lead to the diagnosis of leukemia in these patients. Importantly, we identified five patients with t(17;19)-ALL, and its incidence was estimated to be over 20%, indicating the frequent association of t(17;19) with the development of hypercalcemia in childhood ALL. In all of five t(17;19)-ALL patients in the present study, the leukemia relapsed very early. However, excluding the patients with t(17;19)-ALL, the 5-year EFS rate of ALL accompanied by hypercalcemia was almost similar to that of childhood ALL patients enrolled in TCCSG, indicating that the development of hypercalcemia itself is not a poor prognostic factor in childhood ALL. Thus, identification of t(17;19) is very critical to predict the prognosis of ALL with hypercalcemia.

Among the 21 patients whose PTHrP data were available, the involvement of PTHrP-mediated hypercalcemia was confirmed in 11 patients but ruled out in five patients, indicating that hypercalcemia in childhood ALL is most frequently mediated by PTHrP. The *PTH* and *PTHrP* genes are localized on 11p15.3–15.1 and 12p12.1–11.2, respectively, and none of the patients had detectable chromosomal abnormalities involving these regions in their cytogenetic analysis (Table 1), suggesting that amplification of the regions encoding the *PTH* and *PTHrP* genes might be unlikely as a mechanism for hypercalcemia. Of note, we confirmed the contribution of PTHrP in all three patients with t(17;19)-ALL in whom informative data were available, suggesting that E2A-HLF might induce the production of PTHrP as one of the downstream targets. PTHrP is a potent humoral factor of hypercalcemia, but it was reported that asymptomatic carriers of human T-cell leukemia virus-1 have an elevated serum level of PTHrP without hypercalcemia,[26] suggesting that elevated PTHrP alone might not induce hypercalcemia. We previously reported that E2A-HLF induced the expression of SRPUL, which may play a role in bone invasion as an adhesion molecule.[27] Therefore, frequent association of t(17;19)-ALL with hypercalcemia might result from a synergistic action of PTHrP and SRPUL as downstream targets of E2A-HLF. In contrast, the involvement of PTHrP was specifically ruled out in five patients. Among these five patients, the involvement of PTH in hypercalcemia was strongly suggested in one patient (Case 22) but not in the other four patients (Cases 18–21). Moreover, calcitriol-mediated hypercalcemia, the most frequent cause of hypercalcemia in lymphoma,[4] was unlikely in these four patients. Of note, two patients (Cases 19 and 21) had B-precursor ALL with negative- or low-level expression of CD19 and their serum levels of tumor necrosis factor-α and interleukin-6, which are known to promote osteoclastic bone resorption and involve in hypercalcemia in malignancies,[28,29] were elevated at the onset of hypercalcemia,[30] representing an independent subgroup of ALL with PTHrP-independent hypercalcemia.

In the present study, for the treatment of hypercalcemia, 17 patients received chemotherapy before complete resolution of hypercalcemia, and seven of them received PSL alone. Fifteen patients received calcitonin, 11 patients received bisphosphonates and seven of them received both. Bisphosphonates have been reported to be highly effective for the treatment of hypercalcemia complicated in malignancies with long duration of action by reducing osteoclast viability and inhibiting osteoclast-mediated resorption of bone.[3,31–33] As a first cohort study, we retrospectively confirmed that hypercalcemia resolved quickly in the patients treated with bisphosphonate compared with the patients who were not treated with bisphosphonate. Most of the patients treated with bisphosphonate developed hypocalcemia and almost the half of them required calcium supplementation. Elevated serum creatinine level was observed in two-thirds of our patients, particularly among patients with older age of onset, but was less common among patients with hypophosphatemia. Of importance, treatment of hypercalcemia resolved renal insufficiency and chemotherapy could be started safely. In particular, renal insufficiency rapidly resolved in patients who were treated with bisphosphonate. However, as there was no difference in the final outcome of survival or renal insufficiency between the patients treated with and without bisphosphonate, the usefulness of bisphosphonate in treating hypercalcemia that develops in ALL patients must be confirmed in a future large prospective study.

Table 5 summarizes the characteristics of 12 previously reported cases of t(17;19)-ALL[9–11,14–16,34,35] in addition to five cases identified in the present study. Hypercalcemia developed in 10 of 14 cases: four patients at their original diagnosis and six patients at disease recurrence. There was no association between hypercalcemia and the type of *E2A-HLF* fusion. Twelve of 15 t(17;19)-ALL patients were older than 10 years and eight of 16 patients had accompanying coagulopathy, which is a relatively rare complication in childhood ALL.[13,24] Although no available data in the previously reported cases, it should be noted that all t(17;19)-ALL cases in the present study expressed

Table 5 Characteristics of t(17;19)-ALL

Case	*Age*	*Sex*	*Coagulopathy*	*Hyper calcemia*	*Type of fusion*	*Karyotype at diagnosis*	*Allo BMT in 1stCR*	*Therapeutic outcome*	*Cell line*	*Reference*	*Identification*
1	16	M	+D	+D	Type 1	t(17;19)	ND	Death on 21m	UOC-B1	10	Pt.1
2	15	F	+D	+R	Type 1	t(17;19)	ND	Death on 23m		10	Pt.2
3	17	F	ND	ND	Type 1v	ND	ND	Death on 2.5m	HAL-O1	11	
4	17	F	–	–	Type 2	t(17;19)	Yes	Relapse at 42m		14	Pt.1
5	11	M	–	+D	Type 2	t(17;19)	No	Relapse at 5m		14	Pt.2
6	13	M	–	+R	Type 1+2	ND	No	Relapse at 16m		14	Pt.3
7	ND	ND	–	ND	Type 2	ND	ND	ND		24	DEN-R
8	ND	ND	–	ND	Type 2	ND	ND	ND		24	RFH-N
9	12	F	+D	–	Type 1	Normal	No	Relapse at 5m		34	
10	5	F	+R	+R	Type 2	t(17;19)	No	Relapse at 18m		35	Pt.1
11	5	F	+D	–	Type 2	NA	No	Relapse at 15m		35	Pt.2
12	14	M	+D	–	ND	t(17;19)	No	1stCR untill 12m		35	Pt.3
13	14	F	–	+R	Type 2	t(17;19)	No	Relapse at 9m	Endo-kun	Present Study,[16]	Case 1
14	10	M	+R	+R	Type 1	Normal	No	Relapse at 14m		Present Study	Case 2
15	4	M	–	+D	Type 2	Normal	No	Relapse at 5m	YCU-B2	Present Study,[15]	Case 3
16	14	F	–	+D	Type 1	Add(19)(p13)	No	Relapse at 3m		Present Study,[9]	Case 4
17	12	F	+R	+R	Type 2	Normal	No	Relapse at 2m		Present Study,[16]	Case 5

Abbreviations: ALL, acute lymphoblastic leukemia; Allo BMT, allogeneic bone marrow transplantation, CR, complete remission; D, at diagnosis; F, female; m, month; M, male; ND, not described; R, at relapse; v, variant.

CD33 and three cases had L2 phenotype. Accordingly, older age of onset, coagulopathy, CD33 expression and L2 phenotype in FAB classification in childhood ALL accompanied by hypercalcemia strongly suggest t(17;19)-ALL. In addition to five patients in the present study, almost all of the patients with t(17;19)-ALL relapsed very early. The prognosis of leukemia in the patients who did not develop hypercalcemia (cases 4, 9, 11 and 12 in Table 5) was as poor as that in the patients who developed hypercalcemia at disease onset (cases 1, 5, 15 and 16 in Table 5), indicating that hypercalcemia did not affect prognosis of the patients with t(17;19)-ALL. Of note, one previously reported patient (Case 4 in Table 5) who exceptionally underwent allogeneic bone marrow transplantation (allo-BMT) in the first CR (13 weeks after diagnosis) maintained CR for 42 months,[14] suggesting that allo-BMT performed early in the first CR might prolong the disease-free survival of t(17;19)-ALL patients even if not cured.

Acknowledgements

We thank Masahiro Tsuchida (Department of Pediatrics, Ibaraki Children's Hospital, Mito, Japan) for providing the clinical data of TCCSG and Keiko Kagami (Department of Pediatrics, University of Yamanashi, School of Medicine) for technical supports.

References

1 Mundy GR, Ibbotson KJ, D'Souza SM, Simpson EL, Jacobs JW, Martin TJ. The hypercalcemia of cancer. Clinical implications and pathogenic mechanisms. *N Engl J Med* 1984; **310**: 1718–1727.
2 McKay C, Furman WL. Hypercalcemia complicating childhood malignancies. *Cancer* 1993; **72**: 256–260.
3 Rheingold SR, Lange BJ. Supportive care of children with cancer: Oncology emergencies: Hypercalcemia. In: Pizzo PA and Poplack DG (eds). *Principles and Practice of Pediatric Oncology*, 4th edn. Williams & Wilkins, 2002, pp 1197–1198.
4 Seymour JF, Gagel RF. Calcitriol: the major humoral mediator of hypercalcemia in Hodgkin's disease and non-Hodgkin's lymphomas. *Blood* 1993; **82**: 1383–1394.
5 Burtis WJ, Brady TG, Orloff JJ, Ersbak JB, Warrell Jr RP, Olson BR *et al*. Immunochemical characterization of circulating parathyroid hormone-related protein in patients with humoral hypercalcemia of cancer. *N Engl J Med* 1990; **322**: 1106–1112.
6 Akatsu T, Takahashi N, Udagawa N, Sato K, Nagata N, Moseley JM *et al*. Parathyroid hormone (PTH)-related protein is a potent stimulator of osteoclast-like multinucleated cell formation to the same extent as PTH in mouse marrow cultures. *Endocrinology* 1989; **125**: 20–27.
7 Harutsumi M, Akazai A, Kitamura T, Manki A, Tanaka H, Oda M *et al*. A case of acute lymphoblastic leukemia accompanied with the production of parathyroid hormone-related protein. *Miner Electrolyte Metab* 1995; **21**: 171–176.
8 Hibi S, Funaki H, Ochiai-Kanai R, Ikushima S, Todo S, Sawada T *et al*. Hypercalcemia in children presenting with acute lymphoblastic leukemia. *Int J Hematol* 1997; **66**: 353–357.
9 Shimonodan H, Nagayama J, Nagatoshi Y, Hatanaka M, Takada A, Iguchi H *et al*. Acute lymphocytic leukemia in adolescence with multiple osteolytic lesions and hypercalcemia mediated by lymphoblast-producing parathyroid hormone-related peptide: a case report and review of the literature. *Pediatr Blood Cancer* 2005; **45**: 333–339.
10 Inaba T, Roberts WM, Shapiro LH, Jolly KM, Raimondi SC, Smith SD *et al*. Fusion of the leucine zipper gene HLF to the E2A gene in human acute B-lineage leukemia. *Science* 1992; **257**: 531–534.
11 Hunger SP, Ohyashiki K, Toyama K, Cleary ML. Hlf, a novel hepatic bZIP protein, shows altered DNA-binding properties following fusion to E2A in t(17;19) acute lymphoblastic leukemia. *Genes Dev* 1992; **6**: 1608–1620.
12 Look AT. Oncogenic transcription factors in the human acute leukemias. *Science* 1997; **278**: 1059–1064.
13 Hunger SP. Chromosomal translocations involving the E2A gene in acute lymphoblastic leukemia: clinical features and molecular pathogenesis. *Blood* 1996; **87**: 1211–1224.
14 Devaraj PE, Foroni L, Sekhar M, Butler T, Wright F, Mehta A *et al*. E2A/HLF fusion cDNAs and the use of RT-PCR for the detection of minimal residual disease in t(17;19)(q22;p13) acute lymphoblastic leukemia. *Leukemia* 1994; **8**: 1131–1138.
15 Takahashi H, Goto H, Funabiki T, Fujii H, Yamazaki S, Fujioka K *et al*. Expression of two types of E2A-HLF fusion proteins in YCUB-2, a novel cell line established from B-lineage leukemia with t(17;19). *Leukemia* 2001; **15**: 995–997.
16 Matsunaga T, Inaba T, Matsui H, Okuya M, Miyajima A, Inukai T *et al*. Regulation of annexin II by cytokine-initiated signaling pathways and E2A-HLF oncoprotein. *Blood* 2004; **103**: 3185–3191.
17 Yoshihara T, Inaba T, Shapiro LH, Kato JY, Look AT. E2A-HLF-mediated cell transformation requires both the trans-activation domains of E2A and the leucine zipper dimerization domain of HLF. *Mol Cell Biol* 1995; **15**: 3247–3255.

18 Inukai T, Inaba T, Yoshihara T, Look AT. Cell transformation mediated by homodimeric E2A-HLF transcription factors. *Mol Cell Biol* 1997; **17**: 1417–1424.
19 Inaba T, Inukai T, Yoshihara T, Seyschab H, Ashmun RA, Canman CE *et al*. Reversal of apoptosis by the leukaemia-associated E2A-HLF chimaeric transcription factor. *Nature* 1996; **382**: 541–544.
20 Inukai T, Inaba T, Ikushima S, Look AT. The AD1 and AD2 transactivation domains of E2A are essential for the antiapoptotic activity of the chimeric oncoprotein E2A-HLF. *Mol Cell Biol* 1998; **18**: 6035–6043.
21 Inukai T, Inaba T, Dang J, Kuribara R, Ozawa K, Miyajima A *et al*. TEF, an antiapoptotic bZIP transcription factor related to the oncogenic E2A-HLF chimera, inhibits cell growth by down-regulating expression of the common beta chain of cytokine receptors. *Blood* 2005; **105**: 4437–4444.
22 Smith KS, Rhee JW, Naumovski L, Cleary ML. Disrupted differentiation and oncogenic transformation of lymphoid progenitors in E2A-HLF transgenic mice. *Mol Cell Biol* 1999; **19**: 4443–4451.
23 Honda H, Inaba T, Suzuki T, Oda H, Ebihara Y, Tsuiji K *et al*. Expression of E2A-HLF chimeric protein induced T-cell apoptosis, B-cell maturation arrest, and development of acute lymphoblastic leukemia. *Blood* 1999; **93**: 2780–2790.
24 Hunger SP, Devaraj PE, Foroni L, Secker-Walker LM, Cleary ML. Two types of genomic rearrangements create alternative E2A-HLF fusion proteins in t(17;19)-ALL. *Blood* 1994; **83**: 2970–2977.
25 Tsuchida M, Ikuta K, Hanada R, Saito T, Isoyama K, Sugita K *et al*. Long-term follow-up of childhood acute lymphoblastic leukemia in Tokyo Children's Cancer Study Group 1981-1995. *Leukemia* 2000; **14**: 2295–2306.
26 Yamaguchi K, Kiyokawa T, Watanabe T, Ideta T, Asayama K, Mochizuki M *et al*. Increased serum levels of C-terminal parathyroid hormone-related protein in different diseases associated with HTLV-1 infection. *Leukemia* 1994; **8**: 1708–1711.
27 Kurosawa H, Goi K, Inukai T, Chang KS, Shinjyo T, Rakestraw KM *et al*. Two candidate downstream target genes for E2A-HLF. *Blood* 1999; **93**: 321–332.
28 Tamura T, Udagawa N, Takahashi N, Miyaura C, Tanaka S, Yamada Y *et al*. Soluble interleukin-6 receptor triggers osteoclast formation by interleukin 6. *Proc Natl Acad Sci USA* 1993; **90**: 11924–11928.
29 Kudo O, Fujikawa Y, Itonaga I, Sabokbar A, Torisu T, Athanasou NA. Proinflammatory cytokine (TNFalpha/IL-1alpha) induction of human osteoclast formation. *J Pathol* 2002; **198**: 220–227.
30 Niizuma H, Fujii K, Sato A, Fujiwara I, Takeyama J, Imaizumi M. PTHrP-independent hypercalcemia with increased proinflammatory cytokines and bone resorption in two children with CD19-negative precursor B acute lymphoblastic leukemia. *Pediatr Blood Cancer* 2006, (E-pub aheadof print).
31 Gurney H, Grill V, Martin TJ. Parathyroid hormone-related protein and response to pamidronate in tumour-induced hypercalcaemia. *Lancet* 1993; **341**: 1611–1613.
32 Young G, Shende A. Use of pamidronate in the management of acute cancer-related hypercalcemia in children. *Med Pediatr Oncol* 1998; **30**: 117–121.
33 Lteif AN, Zimmerman D. Bisphosphonates for treatment of childhood hypercalcemia. *Pediatrics* 1998; **102**: 990–993.
34 Daheron L, Brizard F, Millot F, Cividin M, Lacotte L, Guilhot F *et al*. E2A/HLF fusion gene in an acute lymphoblastic leukemia patient with disseminated intravascular coagulation and a normal karyotype. *Hematol J* 2002; **3**: 153–156.
35 Yeung J, Kempski H, Neat M, Bailey S, Smith O, Brady HJ. Characterization of the t(17;19) translocation by gene-specific fluorescent in situ hybridization-based cytogenetics and detection of the E2A-HLF fusion transcript and protein in patients' cells. *Haematologica* 2006; **91**: 422–424.

STEM CELLS
TISSUE-SPECIFIC STEM CELLS

Highly Efficient Ex Vivo Expansion of Human Hematopoietic Stem Cells Using Delta1-Fc Chimeric Protein

TAKAHIRO SUZUKI,[a,b] YASUHISA YOKOYAMA,[c] KEIKI KUMANO,[d] MINOKO TAKANASHI,[e] SHIRO KOZUMA,[f] TSUYOSHI TAKATO,[b,g] TATSUTOSHI NAKAHATA,[h] MITSUO NISHIKAWA,[i] SEIJI SAKANO,[j] MINEO KUROKAWA,[c] SEISHI OGAWA,[a,b] SHIGERU CHIBA[d]

[a]Department of Regeneration Medicine for Hematopoiesis, Graduate School of Medicine, University of Tokyo, Tokyo, Japan; [b]Division of Tissue Engineering, University of Tokyo Hospital, Tokyo, Japan; [c]Department of Hematology and Oncology, Graduate School of Medicine, University of Tokyo, Tokyo, Japan; [d]Department of Cell Therapy and Transplantation Medicine, University of Tokyo Hospital, Tokyo, Japan; [e]The Japanese Red Cross Tokyo Blood Center, Tokyo, Japan; [f]Department of Perinatal Medicine, Graduate School of Medicine, University of Tokyo, Tokyo, Japan; [g]Department of Oral and Maxillofacial Surgery, Graduate School of Medicine, University of Tokyo, Tokyo, Japan; [h]Department of Pediatrics, Graduate School of Medicine, Kyoto University, Kyoto, Japan; [i]Pharmaceutical Division, Kirin Brewery Co., Ltd., Tokyo, Japan; [j]Corporate R&D and Central Research Laboratory, Asahi Kasei Corporation, Tokyo, Japan

Key Words. AC133 antigen • Hematopoietic stem cells • Notch • Stem cell expansion

ABSTRACT

Ex vivo expansion of hematopoietic stem cells (HSCs) has been explored in the fields of stem cell biology, gene therapy, and clinical transplantation. Here, we demonstrate efficient ex vivo expansion of HSCs measured by long-term severe combined immunodeficient (SCID) repopulating cells (SRCs) from human cord blood CD133-sorted cells using a soluble form of Delta1. After a 3-week culture on immobilized Delta1 supplemented with stem cell factor, thrombopoietin, Flt-3 ligand, interleukin (IL)-3, and IL-6/soluble IL-6 receptor chimeric protein (FP6) in a serum- and stromal cell-free condition, we achieved approximately sixfold expansion of SRCs when evaluated by limiting dilution/transplantation assays. The maintenance of full multipotency and self-renewal capacity during culture was confirmed by transplantation to nonobese diabetic/SCID/γc^{null} mice, which showed myeloid, B, T, and natural killer cells as well as $CD133^+CD34^+$ cells, and hematopoietic reconstitution in the secondary recipients. Interestingly, the CD133-sorted cells contained approximately 4.5 times more SRCs than the CD34-sorted cells. The present study provides a promising method to expand HSCs and encourages future trials on clinical transplantation. STEM CELLS *2006;24: 2456–2465*

INTRODUCTION

Umbilical cord blood (CB) is an established stem cell source for hematopoietic stem cell (HSC) transplantation. In many cases, however, CB transplantation is unavailable to patients with relatively high body weight because of the insufficient number of HSCs obtained from a single CB unit [1–3]. Recently, transplantation of multiple units of CB in adult patients was reported in an experimental attempt to infuse a higher number of HSCs or hematopoietic progenitor cells (HPCs), but the effectiveness of this novel trial needs further investigation [4–7].

Another possibility to acquire a higher number of stem cells is ex vivo expansion of HSCs. Although many reports have described potential methods to increase HSCs ex vivo, only a few of them have clearly demonstrated the expansion of long-term severe combined immunodeficient (SCID) repopulating cells (SRCs), currently the only reliable measure of HSCs [8–10]. According to one of these reports, combined use of soluble interleukin (IL)-6 receptor (sIL-6R) and IL-6 together with stem cell factor (SCF), thrombopoietin (TPO), and flt-3 ligand (FL) appeared to be helpful for the successful expansion

Correspondence: Shigeru Chiba, M.D., Ph.D., Department of Cell Therapy and Transplantation Medicine, University of Tokyo Hospital, 7-3-1 Hongo, Bunkyo-ku, Tokyo 113-8655, Japan. Telephone: 81-3-5804-6263; Fax: 81-3-5804-6261; e-mail: schiba-tky@umin.ac.jp; or Seishi Ogawa, M.D., Ph.D., Department of Regeneration Medicine for Hematopoiesis, Graduate School of Medicine, University of Tokyo, 7-3-1 Hongo, Bunkyo-ku, Tokyo 113-8655, Japan. Telephone: 81-3-3815-5411, ext. 35609; Fax: 81-3-5804-6261; e-mail: sogawa-tky@umin.ac.jp Received April 26, 2006; accepted for publication July 11, 2006; first published online in STEM CELLS *EXPRESS* July 20, 2006. 1066-5099/2006/$20.00/0 doi: 10.1634/stemcells.2006-0258

of HSCs, probably because gp130-mediated signals play a critical role in stem cell proliferation and combined use of sIL-6R and IL-6 can transmit signals through gp130 in HSCs, which express gp130 but lack IL-6R [10]. Based on these findings, an artificially generated IL-6/sIL-6R fusion protein, named FP6, which could more efficiently transmit gp130 signals in hematopoietic cells [11], might be a promising agent for ex vivo expansion of HSCs.

Another method that is potentially useful for stem cell expansion is the use of Notch signaling. It is mediated by interactions between transmembrane receptors (Notch1, -2, -3, and -4) and their membrane-bound ligands (Delta and Jagged family molecules). The signaling pathway is known to have differentiation-inhibitory effects in different stem cell systems, including hematopoiesis [12–14]. It has been reported that Notch signaling might play a role in the bone marrow niche, in which Notch ligands are presented by osteoblasts, main components of the niche [15]. In fact, soluble forms of the Notch ligands have been shown to increase immature hematopoietic cells [16–18]. These findings strongly prompt us to use Notch ligands in combination with FP6, for stem cell expansion.

The initial stem cell source is also an important issue for obtaining the maximum efficiency of stem cell expansion. Whereas many investigators use the CD34-sorted cells as a source of stem cell expansion, recent reports suggested that CD133 sorting can concentrate SRCs more efficiently than CD34 sorting [19, 20], and it is still open to question which population is more suitable for stem cell expansion.

In this study, we first addressed the issue of stem cell sources, demonstrating that the CB CD133-sorted cells contained an approximately 4.5-fold greater absolute number of SRCs than CD34-sorted cells. We next evaluated the integrated effect of Notch and gp130 signalings using soluble Delta1 and FP6 in combination with SCF, TPO, FL, and IL-3 and found that this combination could expand human CB CD133-sorted SRCs by 5.8-fold in a serum- and stromal cell-free condition.

MATERIALS AND METHODS

Separation of CD133- and CD34-Enriched Cells from Human CB

Human CB samples were collected from normal full-term deliveries after informed consent was obtained. Mononuclear cells (MNCs) were separated by density gradient centrifugation (Lymphoprep; Axis-shield, Oslo, Norway, http://www.axis-shield.com) after depletion of phagocytes with Silica (Immuno-Biological Laboratories Co., Takasaki, Gunma, Japan, http://www.ibl-japan.co.jp). CD133- and CD34-enriched cells were separated from MNCs by using magnetic cell sorting (MACS) CD133 MicroBead Kit or MACS Direct CD34 Progenitor Cell Isolation Kit (hereafter CD133-MACS and CD34-MACS, respectively; Miltenyi Biotec, Bergisch Gladbach, Germany, http://www.miltenyibiotec.com), respectively. In some experiments, separated cells were examined by flow-cytometric analyses using FcR Blocking Reagent, fluorescein isothiocyanate (FITC)-conjugated anti-human CD34, allophycocyanin (APC)-conjugated anti-human CD133 (clone 293C3) (Miltenyi Biotec), phycoerythrin (PE)-conjugated anti-human CD38 antibodies (BD Pharmingen, San Diego, http://www.bdbiosciences.com/pharmingen), and 7-amino-actinomycin D (7-AAD) (Via-Probe; BD Pharmingen). The yield of the target cells was calculated as follows: [(number of cells after separation) × (purity of the target cells after separation defined by flow-cytometric analysis)] / [(number of MNCs before separation) × (frequency of the target cells among MNCs before separation defined by flow-cytometric analysis)] × 100 (%).

Cytokines

Recombinant human SCF, TPO, IL-3, and IL-6/sIL-6R chimeric protein FP6 were generated by Kirin Brewery Co., Ltd. (Tokyo, http://www.kirin.co.jp/english), and the recombinant Delta1-Fc chimeric protein was generated as previously described [17]. These reagents were certified as free from endotoxin (<0.28 EU/mg protein). Recombinant human IL-6 and FL were purchased from Wako Pure Chemicals (Osaka, Japan, http://www.wako-chem.co.jp/english) and R&D Systems Inc. (Minneapolis, http://www.rndsystems.com), respectively.

Cell Culture

Plates or dishes not treated with tissue culture were precoated with 10 μg/ml Delta1-Fc or control Fc fragment of human IgG (IgG-Fc) (Jackson ImmunoResearch Laboratories, Inc., West Grove, PA, http://www.jacksonimmuno.com) followed by 10 μg/ml human fibronectin (Boehringer Ingelheim GmbH, Ingelheim, Germany, http://www.boehringer-ingelheim.de). Cells were cultured in serum-free medium composed of Iscove's modified Dulbecco's medium (IMDM) supplemented with 10 mg/ml bovine serum albumin, 10 μg/ml human insulin, 200 μg/ml human transferrin, 2 mM L-glutamine, 0.1 mM 2-Mercaptoethanol, 4.7 μg/ml linoleic acid, 4.7 μg/ml oleic acid, and 8 μg/ml cholesterol (Kyokuto Pharmaceutical Industrial Co., Ltd., Tokyo, http://www.kyokutoseiyaku.co.jp) at 37°C in a humidified atmosphere flushed with 5% CO_2 in air. Cytokines were added at concentrations of 100 ng/ml for SCF, 10 ng/ml for TPO, 100 ng/ml for FL, 100 ng/ml for FP6, 100 ng/ml for IL-6, and 10 ng/ml for IL-3. Cell culture was initiated in 24-well plates and serially transferred to six-well plates and 10-cm dishes to avoid overgrowth of the cells. Half of the culture medium was changed every 2 or 3 days.

Colony Assays

At the indicated time points, cultured cells were harvested and plated in a semisolid medium, Methocult GF H4434, containing IMDM with 30% fetal bovine serum (FBS), 0.1 mM 2-mercaptoethanol, 2 mM L-glutamine, 50 ng/ml human SCF, 10 ng/ml human granulocyte-macrophage colony stimulating factor, 10 ng/ml human IL-3, and 3 units/ml human erythropoietin (StemCell Technologies, Vancouver, BC, Canada, http://www.stemcell.com) and incubated at 37°C. Colony-forming ability was assessed after 15–16 days of culture.

Transplantation to Nonobese Diabetic/SCID or Nonobese Diabetic/SCID/γc^{null} Mice

To assess the in vivo repopulating capacity of isolated cells and their cultured progeny, we used nonobese diabetic (NOD)/SCID (NOD/Shi-scid; CLEA Japan, Inc., Tokyo, http://www.clea-japan.com) and NOD/SCID/γc^{null} (NOG) mice [21] (Central Institute for Experimental Animals, Kanagawa, Japan, http://www.ciea.or.jp/English/eindex.htm) as xenotransplantation recipients. Cells separated by CD133-MACS and their cultured

progeny were transplanted intravenously into sublethally irradiated (2.5 Gy using an x-ray irradiator), 8–10-week-old NOD/SCID or NOG mice. When transplanting cells into NOD/SCID mice, we injected intraperitoneally 20 μl of anti-asialo GM1 antibody (Wako Pure Chemicals) diluted in phosphate-buffered saline (PBS) to a total volume of 420 μl immediately before transplantation and on days 11, 22, and 33 after transplantation to reduce the natural killer (NK) cell activity in NOD/SCID mice [10]. Because NOG mice lack intrinsic NK cell activities, administration of anti-asialo GM1 antibody to NOG mice was not needed [21]. Mice were fed with autoclaved acidified water and sterilized food. At 10–13 weeks after transplantation, mice were sacrificed, and cells were harvested from both femurs, peripheral blood, spleen, and thymus. In the indicated experiments, analyses were performed 24 weeks after transplantation. In the limiting dilution transplantation analyses, we transplanted cells into six to 12 recipient mice in each limiting dose for reliable estimation.

In the serial transplantation experiment, we isolated bone marrow cells from the primary NOG recipient mouse 24 weeks after the first transplantation, and MNCs were separated by density gradient centrifugation (Histopaque-1083; Sigma-Aldrich, St. Louis, http://www.sigmaaldrich.com). The MNCs were divided into three aliquots and injected intravenously into secondary NOG recipients. Ten weeks after the second transplantation, bone marrow cells were harvested and analyzed.

Flow-Cytometric Analysis of Transplanted NOD/SCID and NOG Mice

Engraftment of human cells was examined by analyzing human surface antigens using BD LSR2 (Becton, Dickinson and Company, Franklin Lakes, NJ, http://www.bd.com). Cells harvested from the bone marrow, peripheral blood, spleen, and thymus of recipient mice were treated with ammonium chloride red blood cell lysis buffer (Sigma-Aldrich) and blocked with PBS containing 2% FBS, anti-mouse CD16/32 antibody (BD Pharmingen), and FcR Blocking Reagent (Miltenyi Biotec). Then, they were stained with FITC-conjugated anti-human CD45 (clone HI30; BD Pharmingen) and anti-human CD3 (Beckman Coulter, Inc., Fullerton, CA, http://www.beckmancoulter.com), PE-conjugated anti-human CD13, CD33, CD56, CD4 (Beckman Coulter, Inc.), and CD133 (clone 293C3; Miltenyi Biotec), APC-conjugated anti-murine CD45 (clone 30-F11; BD Pharmingen), anti-human CD3, CD19, CD8 (Beckman Coulter, Inc.), and CD34 (Miltenyi Biotec), and 7-AAD (Via-Probe; BD Pharmingen). Successful engraftment of human hematopoietic cells was determined by detection of greater than 0.1% of human $CD45^+$ cells in recipient bone marrow cells.

Limiting Dilution Analysis

The frequencies of SRCs capable of repopulating in NOD/SCID mice were quantified by a limiting dilution analysis by applying Poisson statistics to the single-hit model as described previously [8, 22, 23]. The frequencies of SRCs and statistical comparison between individual populations were calculated by using L-Calc software (StemCell Technologies).

Statistical Analysis

Data are presented as mean ± SEM. Analysis of statistical significance was determined by paired *t* test.

RESULTS

Stem Cell Isolation by the CD133-MACS Recovers a Higher Number of SRCs than by CD34

Because several investigators have suggested that SRCs are more concentrated in $CD133^+$ cells than in $CD34^+$ cells [19, 20], we directly compared the frequency of SRCs contained in the populations sorted by CD133-MACS and CD34-MACS. Flow-cytometric analyses of four CB samples showed that 0.2%–1.4% (mean 0.8%) and 0.8%–3.0% (mean 1.9%) of MNCs were positive for CD133 and CD34, respectively. More than 98% of $CD133^+$ cells were $CD34^+$, and approximately 43% (25%–56%) of $CD34^+$ cells were $CD133^+$ (Fig. 1A, a).

Then, we prepared two identical CB MNC aliquots and isolated CD133- and CD34-enriched cells by CD133- and CD34-MACS. Flow-cytometric analyses after isolation showed that the purities of separated cells were variable among samples (53.1%–93.5% for CD133 and 53.9%–96.3% for CD34), but there was no significant difference between the two separation methods ($p = .12$). Calculated recovery rates of the target cells (see Materials and Methods) were 66% ± 10% for CD133 and 46% ± 10% for CD34, showing a tendency of better recovery of CD133 cells by CD133-MACS than recovery of CD34 cells by CD34-MACS, but the difference was not significant ($p = .06$). After separation, approximately 75% of the CD34-sorted cells were $CD133^+$, whereas virtually all of the CD133-sorted cells were $CD34^+$ with only rare (0.1%) $CD34^-$ cells in most of the samples (Fig. 1A, b and c). Based on the comprehensive calculation, the recovery rates of $CD133^+CD34^+$ cells (i.e., the major SRC-containing population) in the individual samples were 66% ± 10% and 83% ± 8% by CD133- and CD34-MACS separation, respectively. The recovery efficiency of this most immature fraction by CD34-MACS tended to be superior to the one by CD133-MACS, but again it was not significantly different ($p = .14$).

Then, to compare the number of SRCs contained in the populations separated by CD133- and CD34-MACS, we transplanted cells of each population into irradiated NOD/SCID mice intravenously and examined their in vivo hematopoietic repopulating capacity. To evaluate the number of SRCs quantitatively, we transplanted serially reduced numbers of cells. Frequencies of SRCs in the CD133-sorted population were one of 1,454 and 947 in samples 1 and 2, respectively. In contrast, those in the CD34-sorted population were one of 9,306 and 5,904 in samples 1 and 2, respectively (Fig. 1B, 1C). This means that SRCs were sixfold more concentrated in the CD133-sorted population than in the CD34-sorted one. Converting this frequency into the absolute number of SRCs obtained from the same number of primary MNCs, CD133 sorting recovered 308 (sample 1) and 254 (sample 2) SRCs, and CD34 sorting recovered 67 (sample 1) and 59 (sample 2) SRCs from 10^8 of total MNCs (Fig. 1C). Therefore, despite the similar recovery rate of $CD133^+CD34^+$ cells by CD133- and CD34-sorting procedures, CD133 sorting provides 4.3–4.6-fold greater absolute numbers of SRCs than CD34 sorting. Thus, for our subsequent SRC expansion experiments, we used the CD133-sorted population as the culture-initiating cells.

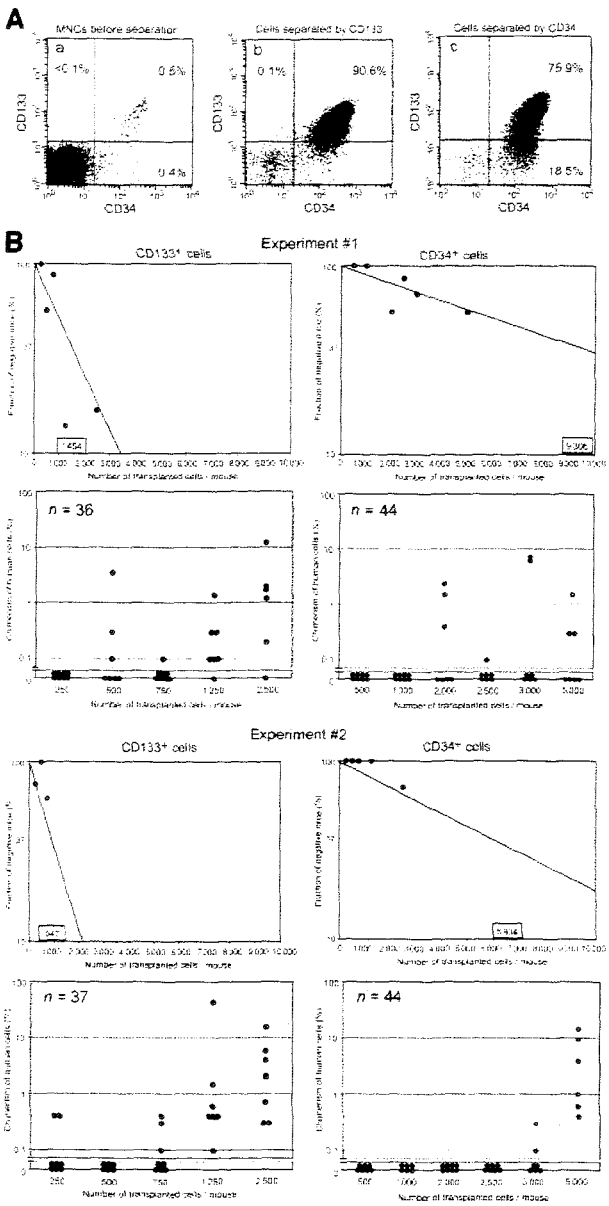

		Frequency of SRCs in the separated population	Number of SRCs in 10^6 of MNCs	Number of SRCs in 10^6 of NCs
Experiment #1	CD133 separation	1 in 1,454	308	741
	CD34 separation	1 in 9,306	67	162
Experiment #2	CD133 separation	1 in 947	254	879
	CD34 separation	1 in 5,904	59	200

Figure 1. Separation of CD133- or CD34-enriched cells from CB MNCs and comparison of their in vivo repopulating capacity. **(A):** Expression profiles of CD133 and CD34 on CB MNCs (a) and cells separated by CD133- (b) and CD34-MACS (c). Representative data among several samples are shown. **(B):** The repopulating ability of CD133- and CD34-sorted cells isolated from the same CB samples (1 and 2). Frequencies of SRCs estimated by limiting dilution analyses are shown. The lower panels show chimeric proportion of human $CD45^+$ cells in the bone marrow of recipient mice, and the number of transplanted mice is shown in the upper-left margin of the panels. **(C):** Estimated frequencies and numbers of SRCs in the transplanted samples. In both experiments, CD133-sorted cells contain higher frequencies of SRCs than CD34-sorted cells, and CD133 sorting provides higher numbers of SRCs from the same volume of original MNCs or NCs than CD34 sorting. Abbreviations: CB, cord blood; MACS, magnetic cell sorting; MNC, mononuclear cell; NC, nucleated cell; SRC, severe combined immunodeficient repopulating cell.

Immobilized Delta1-Fc Chimeric Protein Can Expand Immature CB Hematopoietic Precursors in the Presence of Cytokines

Before evaluating methods for HSC expansion ex vivo, we first explored optimal culture conditions to expand immature hematopoietic precursors by using various combinations of hematopoietic cytokines and soluble Notch ligands. Because immobilization of Notch ligands has been demonstrated to be important for their efficient activity [24, 25], and it has been suggested that immobilized fibronectin fragment CH-296 along with Notch ligands augmented the effect of Notch ligands [24], we immobilized Delta1-Fc chimeric protein on the bottom of the culture plates along with human fibronectin prior to starting culture. We included SCF, TPO, and FL in the culture system as a basal cytokine combination (designated hereafter three growth factors, 3GFs) because these cytokines have been repeatedly shown to be effective for immature HSC/HPC expansion [26].

We cultured CB CD133-sorted cells in four cytokine combinations of (a) 3GFs + IL-6, (b) 3GFs + IL-6 + IL-3, (c) 3GFs + FP6, and (d) 3GFs + FP6 + IL-3, plus additional conditions with Delta1-Fc or IgG-Fc in each cytokine combination, and compared the expansion rate of total cells, $CD133^+$ $CD34^+CD38^-$ immature hematopoietic cells, and mixed colony-forming cells (CFU-Mix). All culture conditions increased the number of total cells and $CD133^+CD34^+CD38^-$ cells during 3-week culture (Fig. 2A, 2B). Addition of IL-3 or replacement of IL-6 with FP6 gave greater expansion of total cells and $CD133^+CD34^+CD38^-$ cells. However, Delta1-Fc had very little effect on the expansion of these cells (Fig. 2A, 2B).

In contrast, addition of IL-3 was always required for the consistent expansion of CFU-Mix until 3 weeks (Fig. 2C). In the presence of IL-3, addition of FP6 increased the number of CFU-Mix significantly better than IL-6 ($p < .01$), recapitulating the previous findings of the lack of IL-6R on immature HPCs [10, 22] and of the requirement of gp130 signaling for the optimal expansion of these immature cells [10, 11]. Regarding the effect of soluble Notch ligands, Delta1-Fc remarkably increased the number of CFU-Mix for a period of 3 weeks, particularly when combined with IL-3 and FP6. Ultimately, the maximum expansion of CFU-Mix was achieved when cells were cultured with 3GFs + FP6 + IL-3 + Delta1-Fc for 3 weeks ($p < .05$) (Fig. 2C).

Effects of IL-6-gp130, IL-3, and Notch Signalings on SRC Expansion in the Serum-Free Culture

We have found that the number of CFU-Mix was continuously increased until 3 weeks in several conditions (Fig. 2C) and declined thereafter (data not shown). And although a previous report demonstrated that serum-containing culture with 3GFs and IL-6/sIL-6R for 1 week increased the number of SRCs by fourfold, no increase of human blood cell chimerism in recipient mice was observed when we cultured cells for 1 week in the serum-free conditions with either 3GFs + FP6 or 3GFs + FP6 + IL-3 + Delta1-Fc (data not shown). Based on these obser-

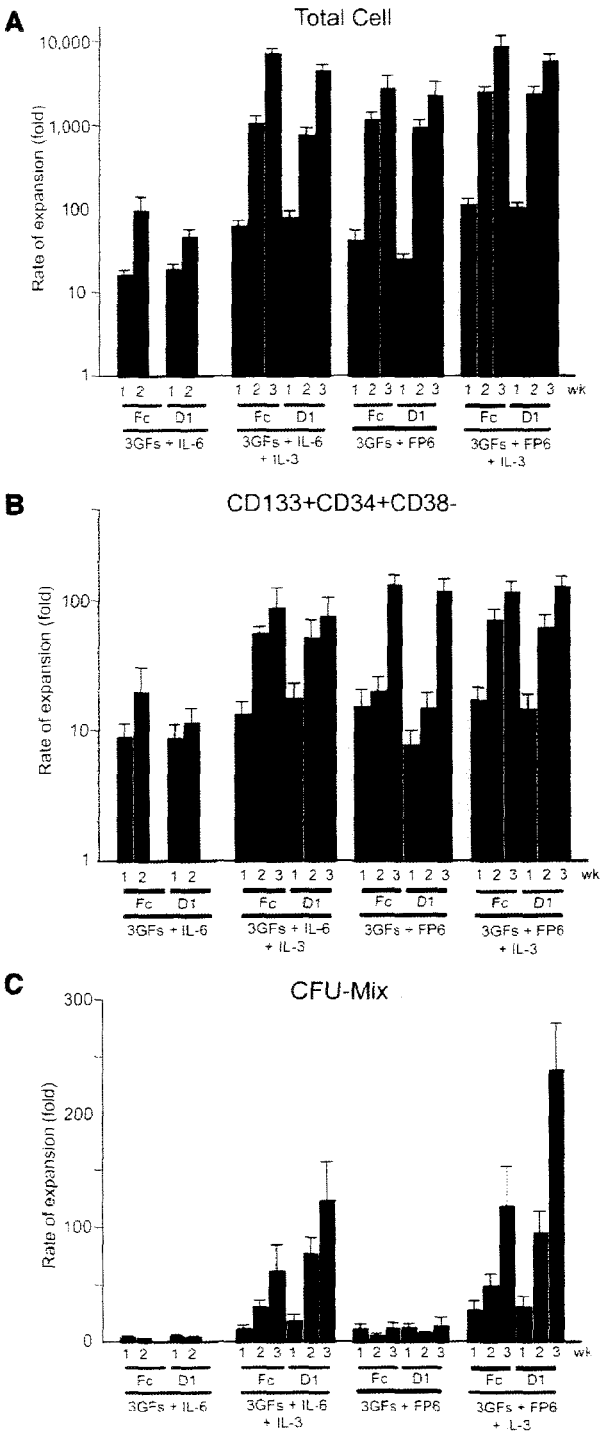

Figure 2. The expansion rates of total cells, $CD133^+CD34^+CD38^-$ immature cells, and CFU-Mix. CB CD133-sorted cells were cultured in the presence of indicated cytokines and Notch ligands for 1, 2, and 3 weeks. **(A, B):** The numbers of total cells **(A)** and $CD133^+CD34^+CD38^-$ immature hematopoietic cells **(B)** were counted, and the expansion rates are shown. **(C):** After indicated periods of culture, cells were replated in a semisolid medium and the number of CFU-Mix was evaluated. The expansion rate of the number of CFU-Mix is shown. Abbreviations: 3GFs, three growth factors; CFU-Mix, mixed colony-forming cells; D1, Delta1-Fc; Fc, IgG-Fc; FP6, interleukin-6/soluble interleukin-6 receptor chimeric protein; IL, interleukin; wk, week.

vations, we determined to culture cells for 3 weeks to evaluate SRC expansion.

As shown in Figure 3A, all the mice transplanted with more than 5,000 fresh CD133-sorted cells showed engraftment, but fewer than 2,500 cells failed to engraft in some of the mice. The frequency of SRCs in this sample was calculated as one of 1,020 (95% confidence interval [CI], 1/548–1/1,899) CD133-sorted cells. Progeny of the CD133-sorted cells grown for 3 weeks with 3GFs + FP6 contained SRCs at a frequency of equivalent to one of 640 (95% CI, 1/414–1/988) culture-initiating cells, and there was no statistical difference between the frequencies of SRCs in these populations, indicating that the addition of FP6–3GFs does not expand SRCs in the serum-free condition ($p = .11$; Fig. 3B), unlike in the serum-containing condition [10].

In contrast, when immobilized Delta1-Fc was present in the same cytokine combination (i.e., 3GFs + FP6), the frequency of SRCs increased to the equivalent to one of 361 (95% CI, 1/218–1/596) culture-initiating cells, indicating 2.8-fold SRC expansion compared with the SRC number before culture ($p = .005$, Fig. 3C). The addition of IL-3 to this condition further augmented the expansion efficiency, achieving the SRC frequency of equivalent to one of 175 (95% CI, 1/109–1/279) culture-initiating cells, indicating 5.8-fold expansion ($p = .0001$, Fig. 3D). To our knowledge, this ranks with the highest human SRC expansion efficiency ever reported. It is of note that two of six mice transplanted with cultured progeny equivalent to 60 culture-initiating cells showed human blood cell chimerism. To further compare the effects of IL-6 and FP6, we replaced FP6 with IL-6. In this condition, SRC frequency was equivalent to one of 266 (95% CI, 1/159–1/446) culture-initiating cells. The expansion rate was reduced from 5.8-fold to 3.8-fold, although significant expansion was still achieved ($p = .0006$; Fig. 3E).

Taken together, significant SRC expansion was realized in all three conditions with immobilized Delta1-Fc chimeric protein. Among these, combination of Delta1-Fc, IL-3, and IL-6/sIL-6R chimeric protein, FP6, in addition to 3GFs, provided the most significant expansion in the serum-free condition. It is noteworthy that IL-3 showed a positive effect in this condition, in contrast to the negative impact in the serum-containing condition without Notch signaling [10].

SRCs Cultured for 3 Weeks in the Serum- and Stromal Cell-Free Condition with 3GFs, FP6, IL-3, and Delta1-Fc Normally Contribute to Myeloid, B, T, and NK Cell Lineages in NOG Recipient Mice and Repopulate Recipients of Secondary Transplantation

To examine the long-term in vivo myeloid and lymphoid repopulating capacity of the cells cultured with 3GFs, FP6, IL-3, and Delta1-Fc, we transplanted these cells into NOG mice, which were generated by intercrossing NOD/SCID mice with IL-2 receptor common γ chain-knockout (γc^{null}) mice. These mice, unlike NOD/SCID mice, are known to allow transplanted human HSCs/HPCs to differentiate even into the T-cell lineage [21], and therefore we could examine the in vivo differentiation capacity of the ex vivo expanded HSCs most efficiently. These mice also have the advantage of higher engraftment of transplanted human cells. We cultured 10,000 CB CD133-sorted cells for 3 weeks and transplanted them into NOG mice. After 12 weeks, we observed 53%–67% human $CD45^+$ cells in the

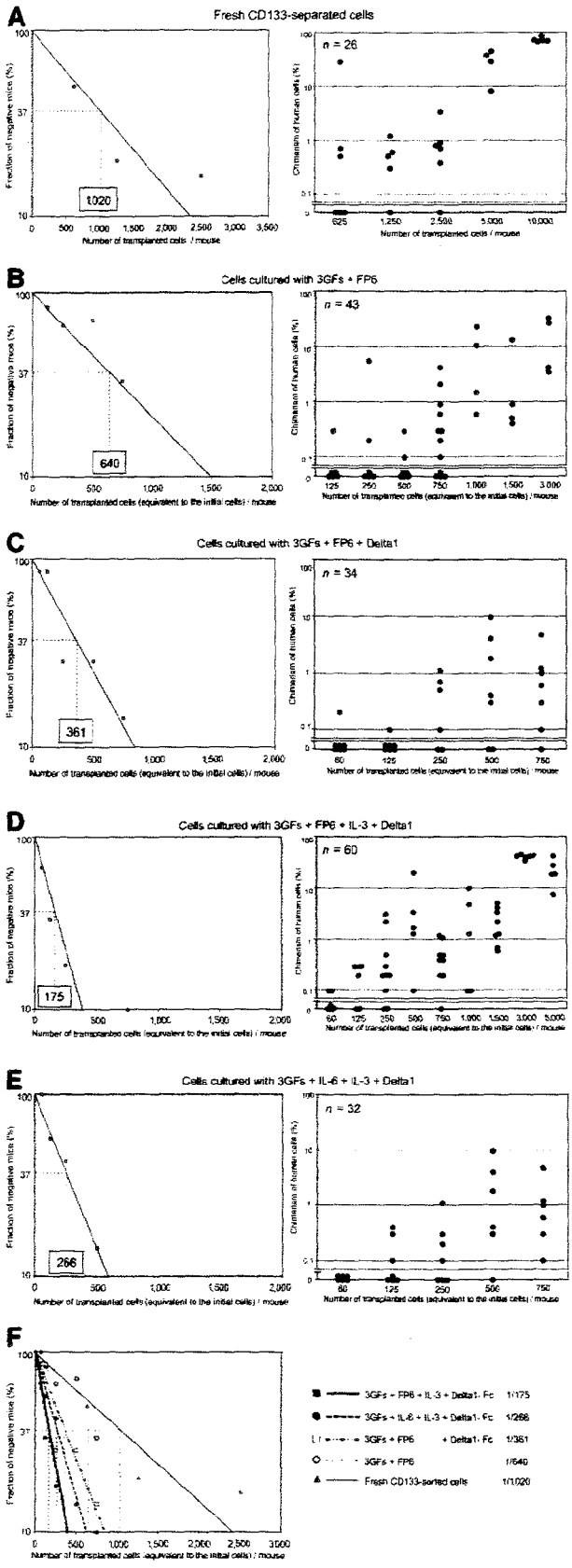

Figure 3. The repopulating ability of fresh CB CD133-sorted cells and their progenies after the culture with various combinations of cytokines for 3 weeks. **(A–E):** The frequencies of SRCs in fresh CD133-sorted cells **(A)**, cells cultured with SCF + TPO + FL (3GFs) + FP6 **(B)**, 3GFs + FP6 + Delta1-Fc **(C)**, 3GFs + FP6 + IL-3 + Delta1-Fc **(D)**, and 3GFs + IL-6 + IL-3 + Delta1-Fc **(E)**. They were estimated as 1/1,020 **(A)**, 1/640 **(B)**, 1/361 **(C)**, 1/175 **(D)**, and 1/266 **(E)**, respectively, by limiting dilution analyses. The right panels show chimeric proportion of human $CD45^+$ cells in the bone marrow of recipient mice, and the number of transplanted mice is shown in the upper-left margin of the panels. **(F):** Integrated representation of **(A–E)**. Correspondence of the symbols and lines is noted in the right. Abbreviations: 3GFs, three growth factors; FL, flt-3 ligand; FP6, interleukin-6/soluble interleukin-6 receptor chimeric protein; IL, interleukin; SCF, stem cell factor; TPO, thrombopoietin.

recipient bone marrow. Further analyses of the bone marrow, peripheral blood, spleen, and thymus of recipient mice revealed that human hematopoietic cells differentiated into myeloid ($CD13^+$ or $CD33^+$), B ($CD19^+$), T ($CD3^+$), and NK ($CD56^+$) cell lineages (Fig. 4A). In addition, in the bone marrow of recipient mice, we detected $CD133^+CD34^+$ immature hematopoietic cells at frequencies of 0.5%–1.1% of human cells. In the thymus, human cells represented virtually all the $CD3^+$ cells (data not shown), and among the $CD3^+$ cells, the patterns of differentiation to CD4/CD8 double-positive, CD4 single-positive, and CD8 single-positive cells were very similar to that of normal thymocytes (Fig. 4A). Robust human hematopoietic repopulation was confirmed in another recipient mouse 24 weeks after transplantation (Fig. 4B). In this mouse, more definite reconstitution of $CD3^+$ mature T cells was observed in the peripheral blood and spleen.

To confirm that transplanted HSCs still retain their self-renewal capacity after primary transplantation, we collected bone marrow cells 24 weeks after the transplantation from a primary recipient, which had been transplanted with the progeny of 1×10^4 CB CD133-sorted cells ex vivo expanded, and injected them into three secondary NOG mice. Ten weeks after the secondary transplantation, we observed engraftment of human $CD45^+$ cells (0.1%) in the bone marrow of two recipient mice (Fig. 5A), and human hematopoietic cells differentiated into myeloid ($CD13^+$ or $CD33^+$) and lymphoid ($CD19^+$) cells (Fig. 5B). These findings strongly indicate that cells cultured with 3GFs, FP6, IL-3, and Delta1-Fc for 3 weeks retain long-term repopulating capacity and normal differentiation capacity in vivo.

DISCUSSION

Efficient Ex Vivo Expansion of SRCs

In this study, we demonstrated successful expansion of SRCs by approximately sixfold, by culturing human CB CD133-enriched cells with SCF, TPO, FL, FP6, IL-3, and Delta1-Fc. SRCs have now been widely accepted as the most immature human hematopoietic cells and are regarded as surrogates for HSCs [26]. In many reports, expansion of SRCs has been discussed by comparison of human blood cell chimerism in recipient mice [16–18, 27–31]. However, to quantify the number of SRCs, limiting dilution/transplantation analyses are essential. Moreover, because the human blood cell chimerism in the bone marrow of recipient NOD/SCID mice typically stabilizes at 10–12 weeks

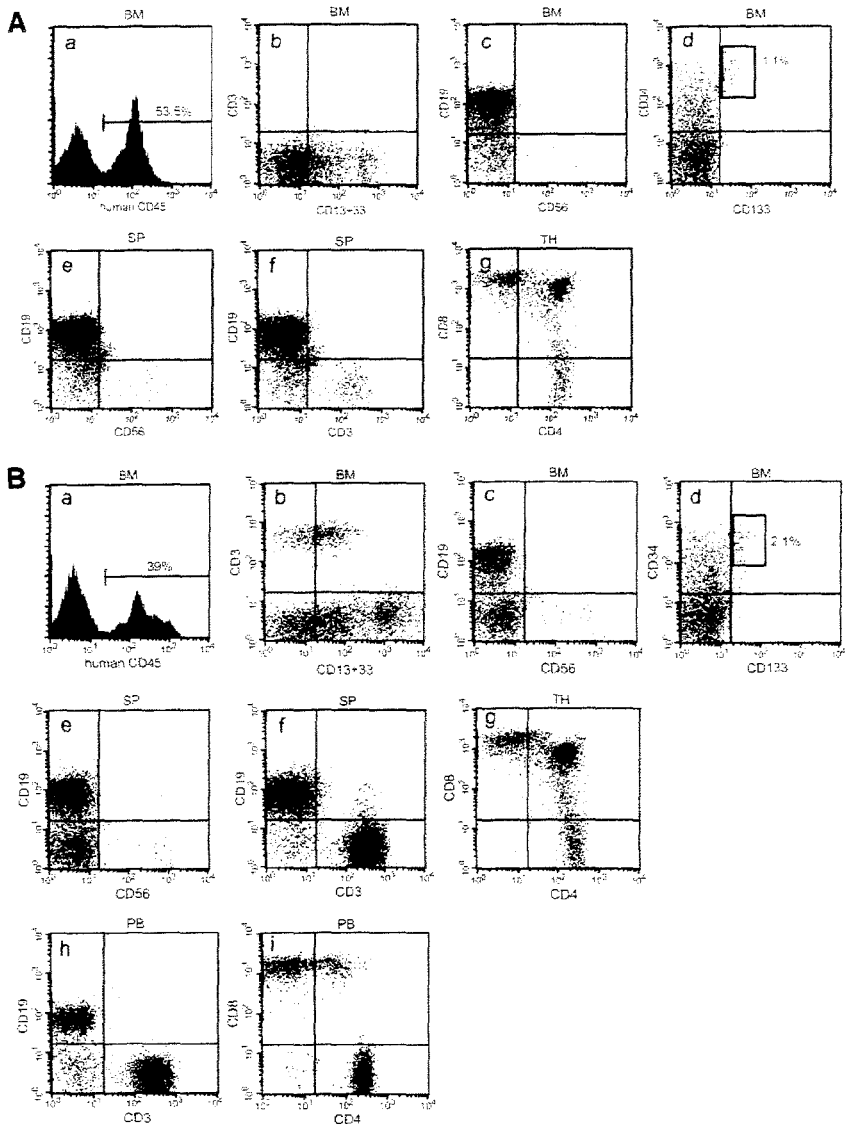

Figure 4. *In vivo repopulating and differentiation capacity of the cells cultured with 3GFs + FP6 + IL-3 + Delta1-Fc.* Cord blood CD133-sorted cells were cultured with 3GFs + FP6 + IL-3 + Delta1-Fc for 3 weeks and were transplanted into NOG mice. The BM, PB, SP, and TH of recipient mice were collected 12 weeks **(A)** and 24 weeks **(B)** after transplantation, and contribution of human cells to various hematopoietic lineages was examined by flow-cytometric analyses. **(A):** Representative data of recipient mice examined 12 weeks after transplantation. Human $CD45^+$ cells accounted for 53.5% of total BM cells (a), and a substantial number of human $CD3^+$ (b, f), $CD13^+$ (b), $CD33^+$ (b), $CD19^+$ (c, e), and $CD56^+$ (c, e) cells were detected in the BM and spleen. $CD133^+CD34^+$ immature hematopoietic cells were also clearly identified (1.1%) in the BM (d). In the thymus, $CD3^+$ cells expressed CD4 and/or CD8 (g) showing a solid development of human T cells. (b–g) represent data gated by human $CD45^+$ cells. **(B):** Flow-cytometric data from a mouse examined 24 weeks after transplantation. A high level of engraftment (a) (39%), reconstitution of $CD133^+CD34^+$ immature cells (d) (2.1%), and contribution to myeloid (b), B-cell (c, e, f, h), T-cell (b, f–i) and NK-cell (c, e) lineages were confirmed in the BM, spleen, thymus, and peripheral blood. (b–i) represent data gated by human $CD45^+$ cells. Abbreviations: 3GFs, three growth factors; BM, bone marrow; FP6, interleukin-6/soluble interleukin-6 receptor chimeric protein; IL, interleukin; NK, natural killer; PB, peripheral blood; SP, spleen; TH, thymus.

after transplantation [32–34], observation for at least 8–10 weeks is optimal to evaluate SRC numbers accurately, and only a few reports have fulfilled these conditions [8–10]. Our analysis, satisfying these criteria, revealed expansion of SRCs, which ranks as the most efficient one. Our method also enabled a 240-fold expansion of CFU-Mix, demonstrating its surprisingly strong effect on expanding immature progenitors.

We also demonstrated that the cultured cells can differentiate in vivo into myeloid, B, T, and NK cell lineages in the bone marrow, peripheral blood, spleen, and thymus in NOG mice. Human cells transplanted into NOG mice can engraft at significantly higher levels than NOD/SCID mice, and transplanted cells can differentiate even to the T-cell lineage. Based on these features, NOG mice are increasingly used as recipients of human stem cells as well as NOD/SCID/β2-microglobulin null mice [21, 35, 36]. We found immature $CD133^+CD34^+$ human cells in the bone marrow of recipient NOG mice at a substantial frequency, and after serial transplantation, progeny of the cultured cells engrafted most of the secondary recipients. These findings suggest that the culture system preserves normal stem cell functions.

Positive Effects of Notch Signaling on SRC Expansion

A positive effect of soluble Notch ligands on human SRCs was previously suggested by two groups, although they did not confirm the increase of SRCs quantitatively [16–18]. In the current study, we have provided clear data that demonstrate that the soluble Notch ligand can truly increase the number of human SRCs ex vivo. There are increasing lines of evidence suggesting that the Notch signaling pathway physiologically plays an important role in maintaining HSCs in the bone marrow niche [15, 37], where the Notch signal might inhibit differentiation of HSCs [15, 37]. Recently, the negative effects of reactive oxygen species for HSC maintenance were discovered [38], and the importance of the low oxygen environment in the HSC niche has been highlighted [39]. Interestingly, maintenance of the undifferentiated state by hypoxia-induced hypoxia-inducible

A

Primary transplant		Secondary transplants			
Cell dose	Human engraftment (%)	Mouse	Transplanted Cell dose	Transplanted Human Cell dose	Human engraftment (%)
cultured cells from 1×10^4 $CD133^+$ cells	24.2	S1	1.1×10^6	2.6×10^5	0.1
		S2	1.1×10^6	2.6×10^5	0
		S3	1.1×10^6	2.6×10^5	0.1

B

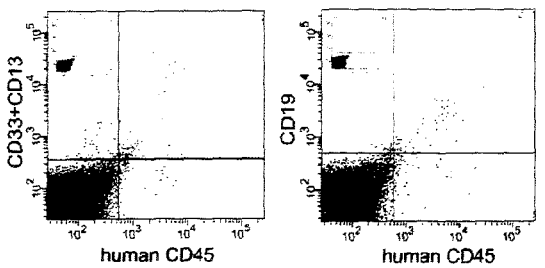

Figure 5. Cells cultured with three growth factors (3GFs) + interleukin (IL)-6/soluble receptor chimeric protein (FP6) + IL-3 + Delta1-Fc retain long-term repopulating capacity after serial transplantation into secondary nonobese diabetic/severe combined immunodeficient/γc^{null} (NOG) recipients. Ten-thousand cord blood CD133-sorted cells were cultured with 3GFs + FP6 + IL-3 + Delta1-Fc for 3 weeks and were transplanted into a primary NOG mouse. Twenty-four weeks after transplantation, bone marrow (BM) cells were harvested and serially transplanted into three secondary NOG recipients. **(A):** Ten weeks after secondary transplantation, BM cells of recipient mice were harvested and chimerism of human cells was analyzed. Two of the three secondary recipients showed substantial human engraftment. **(B):** Representative flow-cytometric data of BM cells in a secondary recipient (mouse S1). Human myeloid ($CD13^+$ or $CD33^+$) and lymphoid ($CD19^+$) cells can be identified. Data with isotype controls are shown as insets in the upper-left margin of the figures.

factor 1α (HIF1α) activation requires Notch signaling, and conversely, Notch signaling is enhanced by activation of HIF1α [39]. It is thus interesting to combine our system with hypoxic conditions for further better efficiency of ex vivo HSC expansion.

Effects of IL-3 and gp130 Signaling Pathways on SRC Expansion

We found that IL-3 exerts positive effects on amplifying SRCs at least in the presence of SCF, TPO, FL, FP6, and Delta1-Fc in a serum-free condition. To date, many researchers have examined the effects of IL-3 on HSCs, but the results have been controversial: some reports showed maintenance of HSCs, whereas others showed negative effects [40]. This discrepancy may depend on the addition of serum, the difference of coexisting cytokines, and the culture-initiating cells. Our result may suggest that IL-3 has additive or synergistic effects with Delta1-Fc on HSCs in the absence of serum.

We also found that replacement of IL-6 with FP6 had some superior effects on SRC expansion. Unlike the addition of IL-3, however, the effects of FP6 were marginal in the presence of Delta1-Fc and IL-3. This could be because the combination of Delta1-Fc and IL-3 could transmit nearly optimal growth signals in HSCs. Or the difference of the cell source (i.e., CD133- vs. CD34-sorted cells) might explain the results [10, 11].

Stem Cell Source for Transplantation and Ex Vivo Culture

To obtain the maximum efficiency of stem cell expansion, the isolation method for culture-initiating cells is also very important. CD34 sorting has been most widely used for positive selection of HSCs in the clinical practice. Recently, feasibility of the CD133-sorted cell transplantation has been evaluated in several clinical trials [41, 42]. There has been, however, no direct comparison of the SRC numbers obtained by these two methods. To the best of our knowledge, most of the CB SRCs are present in the $CD133^+CD34^+$ population [19, 20], and thus, the isolation methods are expected to provide a similar number of SRCs if the separation efficiencies are the same. Surprisingly, however, we found that the absolute SRC numbers were approximately 4.5-fold greater in the CD133-sorted population than in the CD34-sorted one, despite the fact that the recovery efficiency of $CD133^+CD34^+$ cells was very similar. One explanation to this apparently unexpected result could be that CD34, a cell-surface sialomucin protein, might be interfered with by the anti-CD34 antibody used for isolation. Given that accumulating evidence suggests that CD34 regulates homing of the cells to the proper microenvironment after i.v. injection by inhibiting inappropriate cell adhesion [43–45], the anti-CD34 antibody might interfere with the proper homing of the cells by modulating the adhesion capacity. Specifically, we used MACS Direct CD34 Progenitor Cell Isolation Kit for enrichment of $CD34^+$ cells, and this system uses monoclonal antibody QBend10, which recognizes the Class II epitope of the CD34 antigen. The QBend10 and other ClassII antibodies have been shown to induce actin polymerization and enhance cytoadhesiveness of KG-1 cells and primary bone marrow $CD34^+$ cells [46, 47], and this biological property may have reduced the SCID repopulating capacity of the CD34-sorted cells.

Recently, a small population of $CD133^+CD34^-$(Lineage$^-$ [Lin^-]) hematopoietic cells was identified. Because these cells give rise to $CD34^+$ SRCs during culture, $CD133^+CD34^-$ cells might represent precursors of SRCs [48–50]. Therefore, although these cells account for no more than 0.1% of the CD133-sorted cells, the use of CD133-sorted cells as the culture-initiating cells may help increase the absolute number of HSCs after culture.

All these considerations imply that CD133-sorted cells are more advantageous as a direct source for HSC transplantation and as a culture-initiating source for ex vivo HSC expansion than CD34-sorted cells to obtain a greater number of HSCs. According to our results, we can estimate that culturing CD133-sorted cells with Delta1-Fc yields as many as approximately 25-fold greater numbers of HSCs compared with the fresh CD34-sorted cells. Currently, clinical devices for CD34 sorting which use QBend10 or other Class II anti-CD34 antibodies are widely used. Our findings suggest that CD133 sorting might be a better way to collect and enrich HSCs than CD34 sorting by QBend10 or other ClassII antibodies. Future studies that directly compare the clinical outcome of CD133 and CD34 sortings may deepen our understandings for effective enrichment of HSCs.

Conclusion

In this report, we have demonstrated that serum-free culture of the CD133-sorted human CB cells in the presence of SCF, TPO, FL, FP6, IL-3, and Delta1-Fc is an optimized condition to obtain

the highest number of ex vivo expanded HSCs. Based on this condition, some additional explorations should be considered. Increase of differentiated cells surpasses that of immature cells, which might interfere with the SRC expansion because the differentiated cells might secrete various substances that inhibit SRC expansion. Indeed, removal of differentiated cells during culture of CB Lin^- cells has been shown to have strongly positive effect on the efficient SRC expansion in a serum-free culture with 3GFs [51]. Therefore, a much higher level of SRC expansion might be possible if we apply similar differentiated cell-removal protocols in our culture condition. Culture under the hypoxic condition may also improve the expansion efficiency. In this study, we expanded HSCs by a 3-week culture system. In general, shorter ex vivo culture periods are preferable in clinical settings from the viewpoint of safety or costs. Further studies based on our results and above ideas may provide improved methods with shorter culture periods and higher expansion efficiency, which could be the most efficient ex vivo HSC expansion system for clinical applications in the future.

ACKNOWLEDGMENTS

This work was supported by Special Coordination Funds for Promoting Science and Technology from the Ministry of Education, Culture, Sports, Science and Technology of Japan, Research on Pharmaceutical and Medical Safety, Health and Labor Sciences Research Grants from the Ministry of Health, Labor and Welfare of Japan and Grant-in-Aid for Scientific Research, KAKENHI (17014023) from the Japan Society for the Promotion of Science, and a grant from the Takeda Science Foundation. We thank Dr. A. Kikuchi for the supply of CB samples and Kyokuto Pharmaceutical Industrial Co., Ltd. for generously providing us with the serum-free medium. We also thank Y. Sato for taking care of the animals.

DISCLOSURES

M.N. owns stock in and has received financial support from Kirin Brewery Co., Ltd. S.S. owns stock in and has received financial support from Asahi Kasei Corporation.

REFERENCES

1 Benito AI, Diaz MA, Gonzalez-Vicent M et al. Hematopoietic stem cell transplantation using umbilical cord blood progenitors: Review of current clinical results. Bone Marrow Transplant 2004;33:675–690.

2 Chao NJ, Emerson SG, Weinberg KI. Stem cell transplantation (cord blood transplants). Hematology Am Soc Hematol Educ Program 2004: 354–371.

3 Robinson S, Niu T, de Lima M et al. Ex vivo expansion of umbilical cord blood. Cytotherapy 2005;7:243–250.

4 Barker JN, Weisdorf DJ, DeFor TE et al. Rapid and complete donor chimerism in adult recipients of unrelated donor umbilical cord blood transplantation after reduced-intensity conditioning. Blood 2003;102: 1915–1919.

5 Barker JN, Weisdorf DJ, Wagner JE. Creation of a double chimera after the transplantation of umbilical-cord blood from two partially matched unrelated donors. N Engl J Med 2001;344:1870–1871.

6 De Lima M, St John LS, Wieder ED et al. Double-chimaerism after transplantation of two human leucocyte antigen mismatched, unrelated cord blood units. Br J Haematol 2002;119:773–776.

7 Fernandez MN, Regidor C, Cabrera R et al. Cord blood transplants: Early recovery of neutrophils from co-transplanted sibling haploidentical progenitor cells and lack of engraftment of cultured cord blood cells, as ascertained by analysis of DNA polymorphisms. Bone Marrow Transplant 2001;28:355–363.

8 Bhatia M, Bonnet D, Kapp U et al. Quantitative analysis reveals expansion of human hematopoietic repopulating cells after short-term ex vivo culture. J Exp Med 1997;186:619–624.

9 Danet GH, Pan Y, Luongo JL et al. Expansion of human SCID-repopulating cells under hypoxic conditions. J Clin Invest 2003;112:126–135.

10 Ueda T, Tsuji K, Yoshino H et al. Expansion of human NOD/SCID-repopulating cells by stem cell factor, Flk2/Flt3 ligand, thrombopoietin, IL-6, and soluble IL-6 receptor. J Clin Invest 2000;105:1013–1021.

11 Kimura T, Wang J, Minamiguchi H et al. Signal through gp130 activated by soluble interleukin (IL)-6 receptor (R) and IL-6 or IL-6R/IL-6 fusion protein enhances ex vivo expansion of human peripheral blood-derived hematopoietic progenitors. STEM CELLS 2000;18:444–452.

12 Artavanis-Tsakonas S, Rand MD, Lake RJ. Notch signaling: Cell fate control and signal integration in development. Science 1999;284: 770–776.

13 Molofsky AV, Pardal R, Morrison SJ. Diverse mechanisms regulate stem cell self-renewal. Curr Opin Cell Biol 2004;16:700–707.

14 Suzuki T, Chiba S. Notch signaling in hematopoietic stem cells. Int J Hematol 2005;82:285–294.

15 Calvi LM, Adams GB, Weibrecht KW et al. Osteoblastic cells regulate the haematopoietic stem cell niche. Nature 2003;425:841–846.

16 Karanu FN, Murdoch B, Gallacher L et al. The notch ligand jagged-1 represents a novel growth factor of human hematopoietic stem cells. J Exp Med 2000;192:1365–1372.

17 Karanu FN, Murdoch B, Miyabayashi T et al. Human homologues of Delta-1 and Delta-4 function as mitogenic regulators of primitive human hematopoietic cells. Blood 2001;97:1960–1967.

18 Ohishi K, Varnum-Finney B, Bernstein ID. Delta-1 enhances marrow and thymus repopulating ability of human CD34(+)CD38(-) cord blood cells. J Clin Invest 2002;110:1165–1174.

19 de Wynter EA, Buck D, Hart C et al. $CD34^+AC133^+$ cells isolated from cord blood are highly enriched in long-term culture-initiating cells, NOD/SCID-repopulating cells and dendritic cell progenitors. STEM CELLS 1998;16:387–396.

20 Gordon PR, Leimig T, Babarin-Dorner A et al. Large-scale isolation of $CD133^+$ progenitor cells from G-CSF mobilized peripheral blood stem cells. Bone Marrow Transplant 2003;31:17–22.

21 Ito M, Hiramatsu H, Kobayashi K et al. NOD/SCID/gamma(c)(null) mouse: An excellent recipient mouse model for engraftment of human cells. Blood 2002;100:3175–3182.

22 Tajima S, Tsuji K, Ebihara Y et al. Analysis of interleukin 6 receptor and gp130 expressions and proliferative capability of human $CD34^+$ cells. J Exp Med 1996;184:1357–1364.

23 Wang JC, Doedens M, Dick JE. Primitive human hematopoietic cells are enriched in cord blood compared with adult bone marrow or mobilized peripheral blood as measured by the quantitative in vivo SCID-repopulating cell assay. Blood 1997;89:3919–3924.

24 Varnum-Finney B, Wu L, Yu M et al. Immobilization of Notch ligand, Delta-1, is required for induction of notch signaling. J Cell Sci 2000; 113(Pt 23):4313–4318.

25 Vas V, Szilagyi L, Paloczi K et al. Soluble Jagged-1 is able to inhibit the function of its multivalent form to induce hematopoietic stem cell self-renewal in a surrogate in vitro assay. J Leukoc Biol 2004;75:714–720.

26 Heike T, Nakahata T. Ex vivo expansion of hematopoietic stem cells by cytokines. Biochim Biophys Acta 2002;1592:313–321.

27 Angelopoulou M, Novelli E, Grove JE et al. Cotransplantation of human mesenchymal stem cells enhances human myelopoiesis and megakaryocytopoiesis in NOD/SCID mice. Exp Hematol 2003;31:413–420.

28 Lauret E, Catelain C, Titeux M et al. Membrane-bound delta-4 notch ligand reduces the proliferative activity of primitive human hematopoietic $CD34^{+}CD38^{low}$ cells while maintaining their LTC-IC potential. Leukemia 2004;18:788–797.

29 Lemoli RM, Ferrari D, Fogli M et al. Extracellular nucleotides are potent stimulators of human hematopoietic stem cells in vitro and in vivo. Blood 2004;104:1662–1670.

30 Peled T, Mandel J, Goudsmid RN et al. Pre-clinical development of cord blood-derived progenitor cell graft expanded ex vivo with cytokines and the polyamine copper chelator tetraethylenepentamine. Cytotherapy 2004;6:344–355.

31 Shimakura Y, Kawada H, Ando K et al. Murine stromal cell line HESS-5 maintains reconstituting ability of Ex vivo-generated hematopoietic stem cells from human bone marrow and cytokine-mobilized peripheral blood. STEM CELLS 2000;18:183–189.

32 Cashman J, Bockhold K, Hogge DE et al. Sustained proliferation, multilineage differentiation and maintenance of primitive human haemopoietic cells in NOD/SCID mice transplanted with human cord blood. Br J Haematol 1997;98:1026–1036.

33 Coulombel L. Identification of hematopoietic stem/progenitor cells: Strength and drawbacks of functional assays. Oncogene 2004;23: 7210–7222.

34 Pflumio F, Izac B, Katz A et al. Phenotype and function of human hematopoietic cells engrafting immune-deficient CB17-severe combined immunodeficiency mice and nonobese diabetic-severe combined immunodeficiency mice after transplantation of human cord blood mononuclear cells. Blood 1996;88:3731–3740.

35 Kambe N, Hiramatsu H, Shimonaka M et al. Development of both human connective tissue-type and mucosal-type mast cells in mice from hematopoietic stem cells with identical distribution pattern to human body. Blood 2004;103:860–867.

36 Matsumura T, Kametani Y, Ando K et al. Functional $CD5^{+}$ B cells develop predominantly in the spleen of NOD/SCID/gammac(null) (NOG) mice transplanted either with human umbilical cord blood, bone marrow, or mobilized peripheral blood $CD34^{+}$ cells. Exp Hematol 2003; 31:789–797.

37 Duncan AW, Rattis FM, DiMascio LN et al. Integration of Notch and Wnt signaling in hematopoietic stem cell maintenance. Nat Immunol 2005;6:314–322.

38 Ito K, Hirao A, Arai F et al. Regulation of oxidative stress by ATM is required for self-renewal of haematopoietic stem cells. Nature 2004;431: 997–1002.

39 Gustafsson MV, Zheng X, Pereira T et al. Hypoxia requires notch signaling to maintain the undifferentiated cell state. Dev Cell 2005;9: 617–628.

40 Ivanovic Z. Interleukin-3 and ex vivo maintenance of hematopoietic stem cells: Facts and controversies. Eur Cytokine Netw 2004;15:6–13.

41 Bitan M, Shapira MY, Resnick IB et al. Successful transplantation of haploidentically mismatched peripheral blood stem cells using $CD133^{+}$-purified stem cells. Exp Hematol 2005;33:713–718.

42 Lang P, Bader P, Schumm M et al. Transplantation of a combination of $CD133^{+}$ and $CD34^{+}$ selected progenitor cells from alternative donors. Br J Haematol 2004;124:72–79.

43 Drew E, Merzaban JS, Seo W et al. CD34 and CD43 inhibit mast cell adhesion and are required for optimal mast cell reconstitution. Immunity 2005;22:43–57.

44 Healy L, May G, Gale K et al. The stem cell antigen CD34 functions as a regulator of hemopoietic cell adhesion. Proc Natl Acad Sci U S A 1995;92:12240–12244.

45 Krause DS, Theise ND, Collector MI et al. Multi-organ, multi-lineage engraftment by a single bone marrow-derived stem cell. Cell 2001;105: 369–377.

46 Gordon MY, Marley SB, Davidson RJ et al. Contact-mediated inhibition of human haematopoietic progenitor cell proliferation may be conferred by stem cell antigen, CD34. Hematol J 2000;1:77–86.

47 Majdic O, Stockl J, Pickl WF et al. Signaling and induction of enhanced cytoadhesiveness via the hematopoietic progenitor cell surface molecule CD34. Blood 1994;83:1226–1234.

48 Ando K, Nakamura Y, Chargui J et al. Extensive generation of human cord blood CD34(+) stem cells from Lin(-)CD34(-) cells in a long-term in vitro system. Exp Hematol 2000;28:690–699.

49 Bhatia M, Bonnet D, Murdoch B et al. A newly discovered class of human hematopoietic cells with SCID-repopulating activity. Nat Med 1998;4:1038–1045.

50 Gallacher L, Murdoch B, Wu DM et al. Isolation and characterization of human CD34(-)Lin(-) and CD34(+)Lin(-) hematopoietic stem cells using cell surface markers AC133 and CD7. Blood 2000;95: 2813–2820.

51 Madlambayan GJ, Rogers I, Kirouac DC et al. Dynamic changes in cellular and microenvironmental composition can be controlled to elicit in vitro human hematopoietic stem cell expansion. Exp Hematol 2005; 33:1229–1239.

AML1/Runx1 rescues Notch1-null mutation-induced deficiency of para-aortic splanchnopleural hematopoiesis

Masahiro Nakagawa, Motoshi Ichikawa, Keiki Kumano, Susumu Goyama, Masahito Kawazu, Takashi Asai, Seishi Ogawa, Mineo Kurokawa, and Shigeru Chiba

The Notch1-RBP-Jκ and the transcription factor Runx1 pathways have been independently shown to be indispensable for the establishment of definitive hematopoiesis. Importantly, expression of Runx1 is down-regulated in the para-aortic splanchnopleural (P-Sp) region of *Notch1*- and *Rbpsuh*-null mice. Here we demonstrate that Notch1 up-regulates Runx1 expression and that the defective hematopoietic potential of *Notch1*-null P-Sp cells is successfully rescued in the OP9 culture system by retroviral transfer of Runx1. We also show that Hes1, a known effector of Notch signaling, potentiates Runx1-mediated transactivation. Together with the recent findings in zebrafish, Runx1 is postulated to be a cardinal downstream mediator of Notch signaling in hematopoietic development throughout vertebrates. Our findings also suggest that Notch signaling may modulate both expression and transcriptional activity of Runx1. (Blood. 2006;108:3329-3334)

Introduction

Mammalian hematopoietic development is believed to arise from 2 distinct cellular origins. In mice, primitive hematopoiesis arises in the yolk sac (YS) blood island at embryonic day (E) 7.5, while definitive hematopoiesis starts at the ventral region of the aorta-gonad-mesonephros (AGM) around E10.5, which shifts to the liver, spleen, and bone marrow, in this order. Progenitors for definitive hematopoiesis are first detected in the para-aortic splanchnopleural (P-Sp) region at E7.5 to E9.5,[1,2] where the *Notch1* gene has a nonredundant role in hematopoietic stem cell (HSC) development.[3] *Notch1* encodes a 300-kDa heterodimeric single-span transmembrane receptor consisting of a 180-kDa extracellular and a 120-kDa transmembrane subunit. Together with 3 other paralogs, it belongs to the evolutionarily conserved Notch family receptors that mediate cell-fate determination in multiple species. The Notch signaling is initiated by the binding of the Jagged and Delta families of ligands expressed on the neighboring cells, which induces the cleavage of the Notch transmembrane subunit and the release of the Notch intracellular domain. The latter in turn translocates to the nucleus and forms a transactivation complex by interacting with the DNA-binding protein RBP-Jκ and induces the expression of their target genes, such as those for the hairy/enhancer of split (*Hes*) family of basic helix-loop-helix transcription factors.[4] Molecular channels downstream of these, however, are largely unknown.

Mice deficient in *Runx1* (also known as *AML1*, *CBFA2*, or *PEBP2αB*), *Scl*, and *Gata2* genes are lethal during the embryonic stage and show failure in the establishment of definitive hematopoiesis.[5-7] A connection between Notch signaling and these transcription factors has been shown by the analyses of *Notch1*- and RBP-Jκ–encoding *Rbpsuh*-null mice. In the E9.5 P-Sp cells from *Notch1*-null mice, expression levels of SCL, GATA2, and Runx1 mRNA are significantly reduced.[3] *Rbpsuh*-null mice also show markedly reduced levels of SCL, GATA2, and Runx1 mRNA in the endothelial-cell layer of the E9.5 P-Sp region,[8] supporting the notion that the Notch1-RBP-Jκ pathway up-regulates the expression of these key transcription factors. Among these, Runx1, which has close homology to a *Drosophila* protein, Runt, functions as a transcriptional activator or repressor for its target genes in concert with several specific coactivators or corepressors, depending on the context.[9] Importantly, presence of the Notch-Runx pathway has been proposed in *Drosophila* embryonic hemocytogenesis[10] and zebrafish hematopoiesis during both developmental and postnatal periods.[11] Similarly reported has been transcriptional regulation by Notch of the *Gata2* gene in mouse AGM hematopoiesis[8] and of the *Gata* homolog *Serpent* gene in *Drosophila* embryonic hemocytogenesis.[12] In mammals, the existence of Notch-Runx pathway has been unclear.

In this study, we show that Notch1 up-regulates Runx1 mRNA expression in NIH3T3 cells. When introduced to the defective prehematopoietic precursor cells derived from the P-Sp region of *Notch1*-null embryos using retroviruses, Runx1, but neither SCL nor GATA2, restores the definitive hematopoiesis. We also demonstrate that Hes1, one of the Notch signal effectors, augments the transcriptional activity of Runx1 protein. These findings indicate that Runx1 is a key molecule in Notch1-RBP-Jκ–mediated mammalian hematopoiesis.

From the Departments of Hematology and Oncology and Regeneration Medicine for Hematopoiesis, Graduate School of Medicine, University of Tokyo, Japan; and the Department of Cell Therapy and Transplantation Medicine, University of Tokyo Hospital, Tokyo, Japan.

Submitted April 25, 2006; accepted July 3, 2006. Prepublished online as *Blood* First Edition Paper, August 3, 2006; DOI 10.1182/blood-2006-04-019570.

Supported in part by Grant-in-Aid for Scientific Research (KAKENHI no. 17390274) and Grant-in-Aid for Japan Society for the Promotion of Science (JSPS), Fellows from JSPS, Research on Pharmaceutical and Medical Safety, Health and Labour Sciences Research Grants, Ministry of Health, Labour and Welfare of Japan.

The authors declare no competing financial interests.

Reprints: Shigeru Chiba, Department of Cell Therapy and Transplantation Medicine, University of Tokyo Hospital, 7-3-1 Hongo, Bunkyo-ku, Tokyo 113-8655, Japan; e-mail: schiba-tky@umin.ac.jp.

The publication costs of this article were defrayed in part by page charge payment. Therefore, and solely to indicate this fact, this article is hereby marked "advertisement" in accordance with 18 USC section 1734.

Materials and methods

Mice and embryos

C57BL/6 mice were purchased from Japan SLC (Hamamatsu, Japan) and *Notch1* mutant mice[13] were from Jackson Laboratory (Bar Harbor, ME). To generate embryos, timed matings were set up between *Notch1*$^{+/-}$ mice. The time at midday (12 PM) was taken to be E0.5 for the plugged mice.

In vitro P-Sp culture

P-Sp culture was performed as described previously.[14] In brief, isolated P-Sp regions of E9.5 embryos were dissociated by incubation with 250 protease units (PU)/mL dispase (Godo Shusei, Tokyo, Japan) for 20 minutes and cell-dissociation buffer (Gibco BRL, Carlsbad, CA) for 20 minutes at 37°C, followed by vigorous pipetting. Approximately 5×10^4 P-Sp–derived cells were suspended in 300 μL of serum-free StemPro media (Life Technologies, Gaithersburg, MD) supplemented with 50 ng/mL stem-cell factor (SCF), 5 ng/mL interleukin-3 (IL3; gifts from Kirin Brewery, Takasaki, Japan), and 10 ng/mL mouse oncostatin M (R&D Systems, Minneapolis, MN). Single-cell suspensions were seeded on preplated OP9 stromal cells[15] in the 24-well plate, followed by incubation at 37°C in a 5% CO_2 incubator. Images were visualized with a Nikon Eclipse TE2000-U microscope equipped with 40×/0.60 and 10×/0.30 NA objective lenses (Nikon, Tokyo, Japan), and were captured with a C5810 camera (Hamamatsu Photonics, Hamamatsu, Japan).

Plasmid construction

The cDNA of human Runx1 was subcloned into the *Eco*RI restriction site of the retrovirus vector pMYs/internal ribosomal entry site–enhanced green fluorescent protein (IRESEGFP; pMYs/IG).[16] The cDNAs for FLAG-tagged murine SCL and FLAG-tagged murine GATA2 were inserted into the *Eco*RI and *Not*I restriction sites of pMYs/IG. The cDNA for murine Notch1 intracellular domain (NICD)[3] was subcloned into the *Bam*HI restriction site of pMYs/IG. To assess the domain functions of Runx1, we used mutants and wild-type Runx1 constructed in pMY/IG.[14] The pME18S-HA-Runx1 and pME18S-PEBP2β were described previously.[17] The cDNA for FLAG-tagged murine Hes1 was inserted into the *Eco*RI and *Not*I restriction sites of the pME18S-expression vector and in-frame into the *Eco*RI and *Xba*I restriction sites of the p3xFLAG-myc-CMV-25–expression vector (Sigma, St Louis, MO).

Retroviral transduction

Plat-E packaging cells (2×10^6)[16] were transiently transfected with 3 μg of retrovirus vectors, mixed with 9 μL of FuGENE6 (Roche Applied Science, Indianapolis, IN), and incubated at 37°C. Supernatant containing retrovirus was collected 48 hours after transfection and used immediately for infection. Retroviral transduction of the cells derived from *Notch1*-null P-Sp regions was performed as described previously.[14] In brief, the viral supernatant was added to the P-Sp cells seeded on the OP9 stromal-cell layer together with 10 μg/mL polybrene (Sigma). After 72 hours of incubation, virus-containing medium was replaced by the original culture medium. The cells were incubated for another 10 days and processed for analysis. To confirm the expression of proteins, NIH3T3 cells were also infected with the same viral supernatants. The efficiency of infection was evaluated by the positivity of GFP. The proteins were detected by Western blot using anti-Runx1 antibody (PC284L; Oncogene, Cambridge, MA), anti-FLAG monoclonal antibody (M2; Sigma), and anti-FLAG polyclonal antibody (F7425; Sigma) to detect Runx1, GATA2, and SCL, respectively. F7425 antibody was used to exclude the overlap of SCL and nonspecific band by M2 antibody.

CFC assay

The nonadherent or semiadherent cells that emerged from wild-type and *Notch1*-null P-Sp regions were used for colony-forming–cell (CFC) assays. Cells (6×10^4) were plated into MethoCult GF M3434 medium (StemCell Technologies, Vancouver, BC, Canada) and cultured in a 5% CO_2 incubator at 37°C. Colony types were determined at day 7 by morphologic appearance and by Wright-Giemsa staining of each colony. Images were taken with a Nikon Eclipse TE2000-U.

Flow cytometric analysis

Flow cytometric analysis was performed with a BD LSRII (BD Biosciences, San Jose, CA) after addition of 7-amino-actinomycin D (7-AAD) (Via-Probe; BD PharMingen, San Diego, CA) to exclude dead cells. For surface staining, cell suspensions collected from the P-Sp cultures were incubated on ice for 30 minutes in the presence of various mixtures of labeled monoclonal antibodies. The following monoclonal antibodies were purchased from BD PharMingen: phycoerythrin (PE)–conjugated anti–granulocyte 1 (anti-Gr-1), anti–macrophage antigen 1 (anti-Mac-1), anti–stem-cell antigen 1 (anti-Sca-1), anti-Ter-119, allophycocyanin (APC)–conjugated anti-CD45, anti–c-Kit, and biotin-conjugated anti-CD34. Biotinylated antibodies were labeled with PE- or APC-conjugated streptavidin.

Immunoprecipitation and Western blotting

COS7 cells were transfected with expression plasmids (pME-HA-Runx1 and p3xFLAG-myc-CMV-25-Hes1) using the FuGENE6 according to the manufacturer's instruction. The cells were cultured in Dulbecco modified Eagle medium (DMEM) supplemented with 10% fetal calf serum (FCS) for 48 hours after transfection and were lysed in radioimmunoprecipitation assay (RIPA) buffer.[14] These cell lysates were precleared with protein G–sepharose (Amersham Bioscience, Little Chalfont, United Kingdom) and mixed with anti-FLAG antibody (M2; Sigma) or anti-HA antibody (HA.11; Covance Research Products, Berkeley, CA) for 2 hours. The antibody-associated proteins were then recovered on protein G–sepharose beads. The beads were washed 4 times with the RIPA buffer. Whole-cell lysates containing 100 μg of proteins and immunoprecipitates were subjected to 10% sodium dodecyl sulfate–polyacrylamide gel electrophoresis (SDS-PAGE) and transferred to polyvinylidene difluoride membranes (Immobilon; Millipore, Bedford, MA). The membranes were blocked with 5% skim milk treated with either peroxidase-conjugated anti-FLAG monoclonal antibody (M2; Sigma) or peroxidase-conjugated anti-HA monoclonal antibody (12CA5; Roche Applied Science). The blots were visualized using the enhanced chemiluminescence (ECL) system (Amersham Bioscience).

Transcriptional response assays

Luciferase assays were performed as described previously[18] with minor modifications. Briefly, HeLa cells were transfected with 300 ng of reporter (pM-CSF-R-luc),[19] and expression plasmids (combinations of 200 ng of pME18S-HA-Runx1 and 160 ng of pME18S-PEBP2β and 60, 200, or 600 ng of pME18S-FLAG-Hes1 or control) using FuGENE6 according to the manufacturer's instructions. As a control of transfection efficiency, a plasmid expressing β-galactosidase was cotransfected. The cells were harvested 48 hours after transfection and assayed for luciferase activity. The data were normalized to β-galactosidase activity.

Quantitative PCR analysis

NIH3T3 cells were infected with NICD or mock retrovirus. The cells were cultured in DMEM medium supplemented with 10% FCS for 48 hours after infection and were selected by the expression of GFP with the FACSAria (BD Biosciences). Total cellular RNA was extracted with RNeasy (QIAGEN, Hilden, Germany) and converted into cDNAs by reverse transcriptase (Superscript III; Invitrogen, Carisbad, CA). Real-time polymerase chain reaction (PCR) was performed using TaqMan Gene Expression Assays Mm00486762_m1 (Applied Biosystems, Foster City, CA) with the ABI PRISM 7000 Sequence Detection System (Applied Biosystems) according to the manufacturer's instructions. Amplification of 18S ribosomal RNA cDNA was used as the endogenous normalization standard.

Results

Retroviral expression of Runx1 rescues hematopoietic defects of *Notch1*-null P-Sp regions

It has been reported that expression of Runx1 or its homolog, *Lozenge*, is up-regulated by positive Notch signaling in zebrafish and *Drosophila* systems, respectively.[10,11] We thus first evaluated whether Notch activation results in up-regulation of Runx1 also in the mammalian system. When NIH3T3 cells were transiently transfected with Notch1 intracellular domain (NICD), which represents the constitutive active form of Notch1, the mRNA level of Runx1 increased (Table 1).

We then examined whether forced expression of Runx1 could rescue the hematopoietic defect of *Notch1*-null mice. Wild-type P-Sp cells gave rise to round-shaped nonadherent cells when overlayed on the OP9 stromal cells. Flow cytometric analysis of these cells revealed that they were viable (7-AAD negative) CD45-positive cells (top panels in Figure 1A), representing hematopoietic cells. No such cells were generated from *Notch1*-null P-Sp cells and only background OP9 cells were observed (bottom panels in Figure 1A).[3] We retrovirally infected *Notch1*-null P-Sp cells that were seeded on the OP9 layer with Runx1, SCL, or GATA2, and assessed whether *Notch1*-null P-Sp cells could generate hematopoietic cells. Titers of the retroviruses containing Runx1, SCL, and GATA2 were similar to each other as evaluated by infecting NIH3T3 cells with these viruses (Figure 2A). Expression of individual proteins was confirmed by a Western blot analysis (Figure 2B). Mock, SCL, and GATA2 transduction did not generate round-shaped nonadherent cells morphologically or viable CD45-positive cells detectable by flow cytometric analysis. In contrast, Runx1-transduced P-Sp cells gave rise to round-shaped nonadherent cells. These cells were shown to be viable CD45-positive cells by flow cytometric analysis (Figure 1B). This pattern was identical to the positive control (Notch1$^{+/+}$ P-Sp cells; top panels in Figure 1A).

To confirm that the cells developed from Runx1-infected *Notch1*-null P-Sp cells (hereafter referred to as Runx1-rescued cells) retain the features of hematopoietic cells, we evaluated these cells for surface markers and CFC activities. The flow cytometric analysis of the Runx1-rescued cells at day 12 revealed that they express hematopoietic cell-surface markers such as a panleukocyte marker (CD45), stem-cell markers (c-Kit, CD34, and Sca1), myeloid-cell markers (Gr-1 or Mac-1), and an erythroid-cell marker (Ter-119) (Figure 3A). Their expression profiles were reminiscent of those of hematopoietic cells generated from the wild-type P-Sp cells (Figure 3B). The P-Sp culture system faithfully reproduced the generation of hematopoietic cells, and there were no consistent differences between Runx1-rescued and wild-type P-Sp–derived cells in the surface-marker expression levels, although we observed variable minor differences in individual experiments partly because of the variation in the time required for hematopoietic development (Figure 3A-B).

When the Runx1-rescued cells were seeded into semisolid medium at day 12 and cultured for an additional 7 days, they generated mixed, granulocyte/macrophage, and erythroid colonies containing enucleated erythrocytes (Figure 4A) at a frequency comparable to that of wild-type P-Sp–derived cells (Figure 4B-C). There were no statistical differences in the numbers of total ($P = .11$) and individual (erythroid, $P = .20$; granulocyte/macrophage, $P = .11$; mixed, $P = .07$) colonies generated from *Notch1*$^{+/+}$

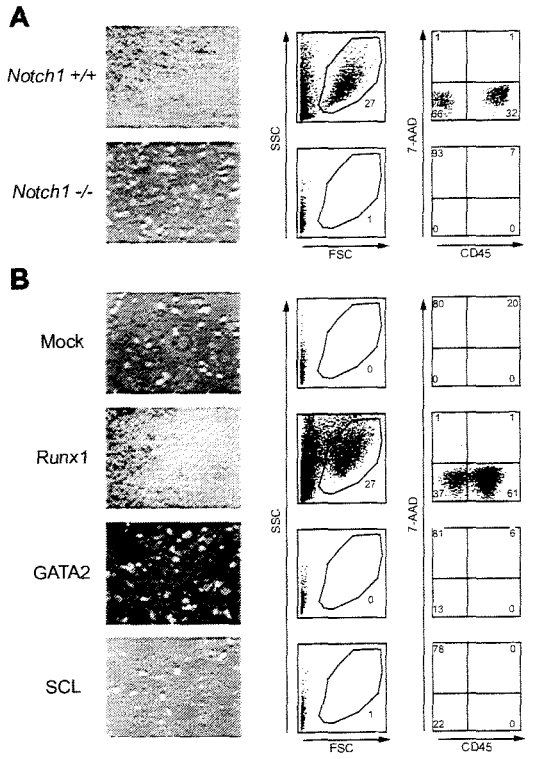

Figure 1. Retroviral expression of Runx1 rescues hematopoietic defect of *Notch1*-null P-Sp region. (A) P-Sp cells from wild-type (*Notch1*$^{+/+}$) and *Notch1*-null (*Notch1*$^{-/-}$) embryos at E9.5 were cultured for 5 days on OP9 cells. (B) P-Sp cells from *Notch1*-null embryos at E9.5 were infected with mock retrovirus or retrovirus containing Runx1, SCL, or GATA2, and cultured for 12 days on OP9 cells. Microscopic representation (left column; original magnification, × 100). Only cocultured OP9 cells are shown if hematopoietic cells are not produced. Flow cytometric analyses (center and right columns) of cells generated in the culture. Percentages of cells gated (center columns) and cells in each quadrant (right columns) are indicated.

Table 1. Notch activation up-regulates the expression of Runx1

	RAU	Mean	Notch-mock
Experiment 1			2.78*
NIH3T3-Mock	0.112634; 0.077514; 0.093663	0.094604	
NIH3T3-Notch	0.263982; 0.241864; 0.282636	0.262827	
Experiment 2			4.12*
NIH3T3-Mock	0.038500; 0.045755; 0.044123	0.042792	
NIH3T3-Notch	0.186016; 0.148638; 0.194443	0.176366	

Data are from 2 independent experiments in triplicate. RAU, relative arbitrary units; Notch-mock, the ratio of RAU by constitutive active Notch 1 infection and RAU by mock infection.

*$P < .01$ (2-tailed, unequal variance t test).

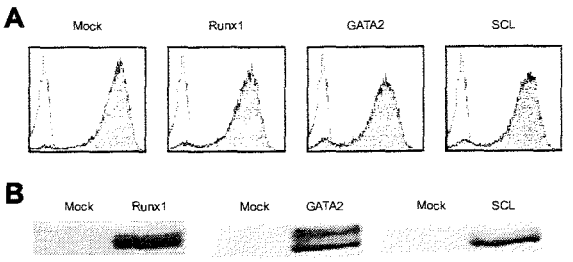

Figure 2. Retroviruses properly create Runx1, GATA2, and SCL proteins. (A) The efficiency of retrovirus-mediated gene transfer of Runx1, GATA2, or SCL was estimated by infecting NIH3T3 cells. Retrovirus-infected cells were evaluated by the expression of GFP (shaded histograms). Uninfected NIH3T3 cells are also shown as a control (open histograms). (B) Expression of individual proteins was confirmed by a Western blot analysis.

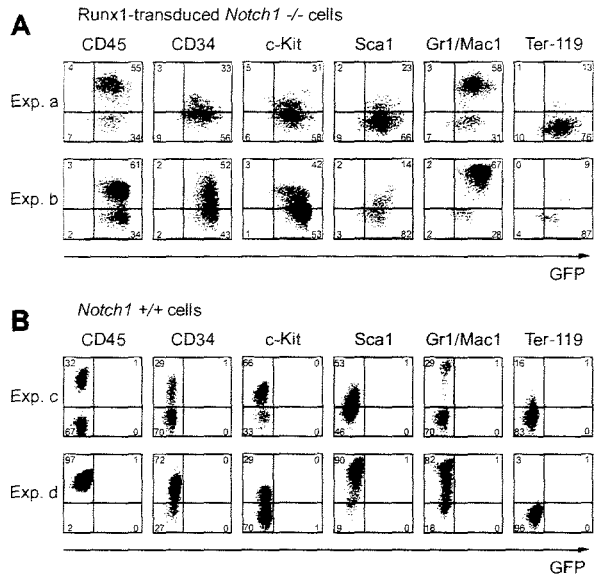

Figure 3. Runx1-rescued cells express hematopoietic surface markers. Expression of hematopoietic surface markers of cultured cells at day 12 from Runx1-transduced *Notch1*-null (*Notch1*$^{-/-}$) embryos (A) or wild-type (*Notch1*$^{+/+}$) embryos (B) was evaluated by flow cytometric analyses. GFP intensity (marking retrovirus-transduced cells) is plotted on the x-axis and intensity of counterstaining of hematopoietic surface markers is plotted on the y-axis. The results show representative results of independent replicates from 5 experiments. Percentages of cells in each quadrant are indicated.

and Runx1-transduced *Notch1*$^{-/-}$ P-Sp–derived cells. These observations indicate that the hematopoietic characteristics of Runx1-rescued cells were similar to those of wild-type P-Sp–derived cells.

Functional implication of Runx1 at the downstream of Notch-RBP-Jκ pathway

Runx1 has several distinct domains with defined biochemical functions. The Runt domain mediates both binding to DNA and dimerization with a partner protein, CBFβ/PEBP2β, whereas the transactivation domain interacts with transcriptional coactivators. Inhibitory domain counteracts the effect of the transactivation domain. The VWRPY motif located near the C-terminus mediates the interaction with a corepressor, TLE. A domain that interacts with mSin3A corepressor is also identified.[9] To assess whether Runx1 functions as an activator or a repressor[20] to restore the hematopoietic defect of *Notch1*-null embryo, we examined a series of Runx1 mutants (Figure 5)[14] for hematopoietic rescue.

Infection of retroviruses containing wild-type and several mutants, Δ444, Δ397, and Δ205-332 of Runx1 (Figure 5) resulted in the rescue of the *Notch1*-null phenotype, giving the same pattern with the culture of wild-type P-Sp cells (Figure 1A, top panels). In contrast, other mutants, Δ335, Δ288, AML1a, ΔRD, Δ205-332, and R139G (Figure 5) could not rescue the *Notch1*-null phenotype, giving the same pattern with the negative control (Figure 1A, bottom panels). Therefore, wild-type of Runx1 and the mutants that lack the VWRPY domain (Δ444, Δ397) or the mSin3A-binding region (Δ181-210) could restore the production of hematopoietic cells in the *Notch1*-null P-Sp culture, whereas those mutants that lack transactivation domain (Δ335, Δ288, AML1a, and Δ205-332) or Runt domain (ΔRD) could not rescue hematopoiesis from the *Notch1*-null P-Sp cells. Since changes in the tertiary structure of the protein could influence the function independent of the role of each domain, we also examined R139G, a mutant isolated from a patient with myelodysplastic syndrome (MDS) that harbors a point mutation causing substitution of Arg139 in the Runt domain with Gly. The DNA-binding ability is severely impaired in R139G, although the ability to heterodimerize with CBFβ/PEBP2β is spared.[21] This mutant could not restore hematopoiesis. These results suggest that, in the presence of an intact Runt domain, the transcriptional activating function is necessary and sufficient for Runx1 to rescue the hematopoietic defect of *Notch1*-null mice in the P-Sp culture system, while the transcriptional repressing function is dispensable.

Notch signaling also regulates transactivating function of Runx1

Hes1 is known to be a canonical Notch-RBP-Jκ target gene in mammals. It is also evident, however, by a number of studies that Hes1 mediates a part of, but not the whole, Notch-RBP-Jκ signaling.[22] In adult hematopoiesis, Hes1 maintains HSCs in vitro and expands them in vivo when retrovirally introduced to a highly HSC-enriched population.[23] Because Hes1 is expressed in the hematopoietic clusters budding from the dorsal aorta,[8] this transcription factor is a candidate as a physiologic target of the Notch-RBP-Jκ pathway in the embryonic hematopoietic development. Hes1 has also been known to mediate cross-talk between Notch and

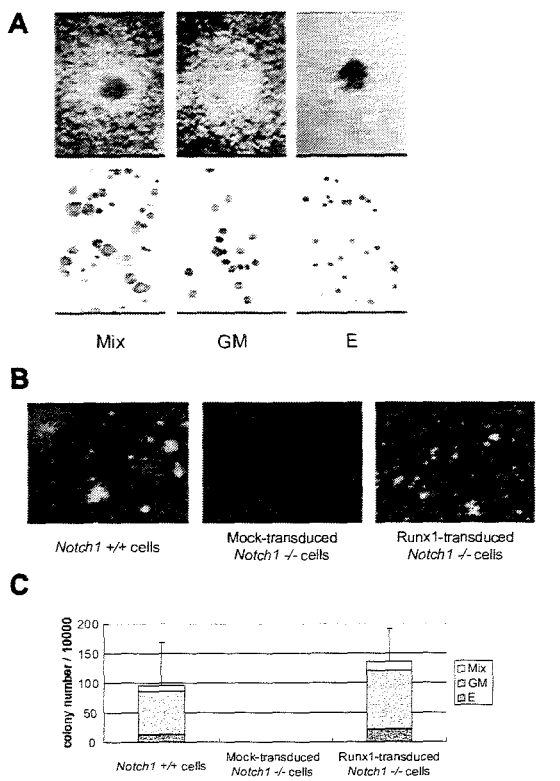

Figure 4. Runx1-rescued cells generate hematopoietic colonies. Colony formation of the Runx1-rescued cells from *Notch1*-null embryos. The rescued cells were harvested at day 12 and plated into MethoCult GF M3434 medium. (A) Representative hematopoietic colonies at day 7 are shown. Mix indicates mixed colony; GM, granulocyte/macrophage colony; and E, erythroid colony. Morphology of the colonies (top panels); original magnification, × 100. Wright-Giemsa–stained cytospin preparation of corresponding cell populations (bottom panels); original magnification, × 600. (B) Photographs of representative colonies. Original magnification, × 3. (C) The total number of colonies and the frequencies of different kinds of colonies. The results show the mean values of 5 independent experiments, each in duplicate, with standard deviations for the total colony numbers. Data were statistically analyzed by 2-tailed, unequal-variance *t* test.

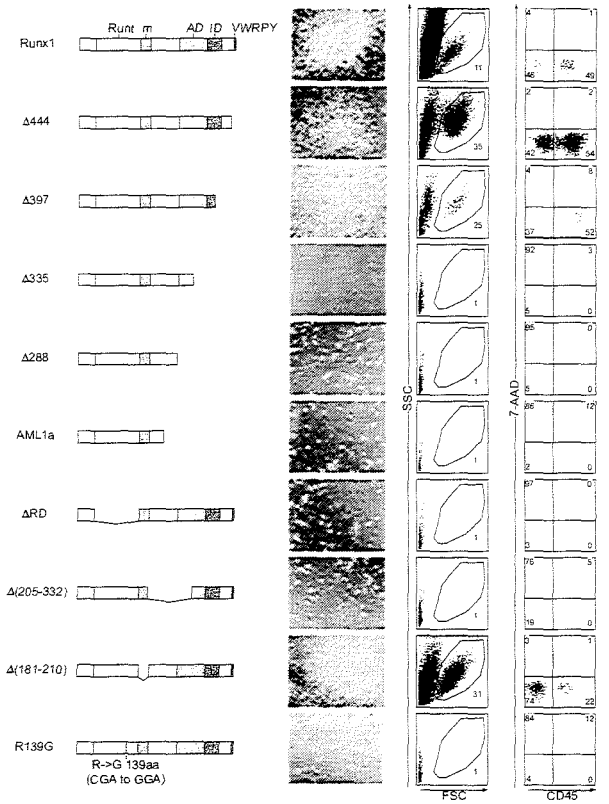

Figure 5. The transcriptionally active form of Runx1 is required for hematopoietic rescue. P-Sp cells from *Notch1*-null embryos at E 9.5 were infected with retroviruses containing *Runx1* mutants and cultured on OP9 cells for 12 days. Structures of Runx1 mutants are depicted (left column). Runt indicates the Runt domain; m, a binding region for mSin3A; AD, transactivation domain; ID, inhibitory domain; and VWRPY, VWRPY motif. Microscopic representations (center column; original magnification, × 100) and flow cytometric analyses (right 2 columns) of cells produced in the culture. Percentages of cells gated (center columns) and cells in each quadrant (right columns) are indicated.

other signaling pathways such as Janus-activating kinase/signal transducer and activator of transcription (JAK/STAT), Wnt, and Ras/mitogen-activated protein kinase (MAPK) pathways.[24-26] Furthermore, the transactivating function of Runx2, another Runx family member, is modified by Hes proteins and their relatives Hey proteins. When overexpressed, Hes1 potentiates Runx2-mediated transactivation in the transfected cells,[27] while Hey represses Runx2-mediated transactivation.[28,29]

Based on these pieces of information, we assessed whether Hes1 also modulates Runx1-mediated transactivation. Consistent with a previous report in which Hes1 was shown to bind to Runx1 in glutathione S-tranferase (GST) pull-down assays,[27] we detected HA-tagged Runx1 protein in the anti-FLAG immunoprecipitant, and reversely, FLAG-tagged Hes1 protein in the anti-HA immunoprecipitant, indicating physical interaction of Hes1 with Runx1 (Figure 6A). Moreover, Hes1 potentiated Runx1-mediated transactivation when expressed in HeLa cells, depending on the expression levels of Hes1 (Figure 6B).

Discussion

In this study, we showed that Runx1 rescues the defective hematopoiesis of *Notch1*-null mice in the OP9 culture system. The functional relationship between Notch and Runx families during hematopoietic development was first indicated in *Drosophila*, in which Notch up-regulates the expression of a *Runt* family gene, *Lozenge*.[10] More recently, it was shown that a zebrafish Notch-signaling mutant *mind bomb* fails in the specification of definitive HSCs during embryogenesis, and that Runx1 is required for expansion of HSCs in the zebrafish AGM region sufficient to restore the HSC specification in the *mind bomb* mutant.[11] The data shown in the present study strongly indicate that the Notch-Runx pathway is conserved from invertebrates to mammals and that Runx1 locates at a very proximal position in the Notch1 signaling pathway during establishment of definitive hematopoiesis.

GATA2 is also reported to have an important role downstream of Notch signaling in the establishment of definitive hematopoiesis. It was reported that NICD directly binds to the *Gata2* promoter and increases its expression level in mouse AGM cells.[8] Similarly in *Drosophila*, Notch up-regulates *Serpent* and induces emergence of hemocyte progenitors in lymph glands.[12] In our retroviral expression system, however, GATA2 could not rescue the hematopoietic defect of *Notch1*-null P-Sp cells (Figure 1B). It remains unknown whether GATA2 expression in more regulated levels and/or timings could rescue the hematopoietic deficient phenotype of *Notch1*-knockout P-Sp cells.

We clearly demonstrated that definitive hematopoiesis is rescued by forced expression of Runx1 in the *Notch1*-null P-Sp cells, but it should be directly shown whether transplantable HSCs are generated from the *Notch1*-null Runx1-introduced P-Sp cells. Fresh P-Sp cells obtained from wild-type embryos can be engrafted

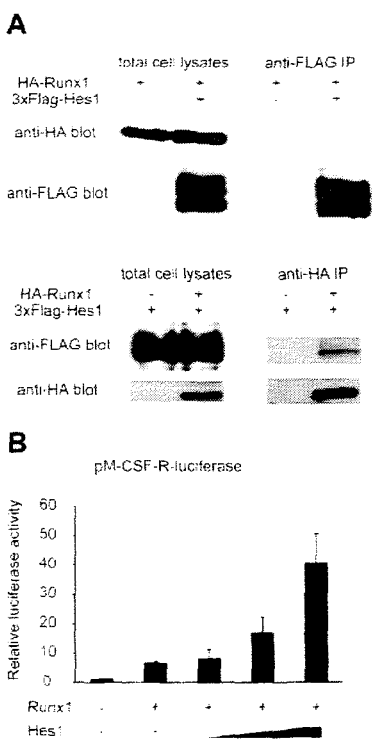

Figure 6. Notch signaling regulates transcriptional level of Runx1 and modulates the function of Runx1 protein through the effector protein, Hes1. (A) COS7 cells were transfected with HA-tagged Runx1 and 3xFLAG-tagged Hes1. Whole-cell extracts were immunoprecipitated (IP) with anti-FLAG antibody or anti-HA antibody followed by immunoblotting (blot) using anti-HA antibody or anti-FLAG antibody. (B) Relative luciferase activity in HeLa cells transfected with Runx1 (200 ng) and Runx1-dependent macrophage colony-stimulating factor receptor (pM-CSF-R) luciferase reporter (300 ng) with or without cotransfection of Hes1 (60, 200, or 600 ng). Data are means ± standard errors of duplicate wells in a representative experiment. Reproducible results were obtained in 3 independent experiments.

to mouse bone marrow if injected in the preconditioned newborn mice, as described.[3,30] It is unknown, however, whether the cultured P-Sp cells are also engraftable with the same method. We were unable to observe engraftment of the cultured P-Sp cells unlike fresh P-Sp cells, when injected to busulfan-pretreated newborn mice (data not shown). Culturing the cells, even for just a short time, is prerequisite for the retroviral gene transfer, which stands as a major technical obstacle to assess the engraftability of the *Notch1*-null Runx1-introduced P-Sp cells. Transgenic expression of Runx1, under an appropriate promoter, in the *Notch1*-null background may reveal further that the Notch1-Runx1 pathway represents an essential physiologic channel for the mammalian HSC generation from the P-Sp cells.

We also showed that Hes1, a known mediator of Notch signaling, cooperatively activates the Runx1-responsive pM-CSF-R luciferase reporter. This observation suggests that the Notch1 pathway modulates expression of Runx1 target genes through multiple mechanisms. There is a possibility that Notch1 directly augments the expression of Runx1 target genes. Although overexpression of Runx1 is sufficient to restore hematopoietic potential in *Notch1*-null P-Sp cells, both of these mechanisms might cooperatively contribute to HSC generation during normal development.

Acknowledgments

We thank M. Ohki for the gift of the human Runx1 cDNA, Y. Ito for the PEBP2β cDNA, D.-E. Zhang for the pM-CSF-R-luc vector, T. Kitamura for the Plat-E packaging cells and the pMYs/IRES-EGFP retrovirus vector, T. Nakano for the OP9 stromal cells, R. Kageyama for the Hes1 cDNA, and Kirin Brewery Pharmaceutical Research Laboratory for the cytokines. We dedicate this paper for the late Prof Hisamaru Hirai, who passed away during the progress of this study.

References

1. Cumano A, Dieterlen-Lievre F, Godin I. Lymphoid potential, probed before circulation in mouse, is restricted to caudal intraembryonic splanchnopleura. Cell. 1996;86:907-916.
2. Godin IE, Garcia-Porrero JA, Coutinho A, Dieterlen-Lievre F, Marcos MA. Para-aortic splanchnopleura from early mouse embryos contains B1a cell progenitors. Nature. 1993;364:67-70.
3. Kumano K, Chiba S, Kunisato A, et al. Notch1 but not Notch2 is essential for generating hematopoietic stem cells from endothelial cells. Immunity. 2003;18:699-711.
4. Artavanis-Tsakonas S, Rand MD, Lake RJ. Notch signaling: cell fate control and signal integration in development. Science. 1999;284:770-776.
5. Okuda T, van Deursen J, Hiebert SW, Grosveld G, Downing JR. AML1, the target of multiple chromosomal translocations in human leukemia, is essential for normal fetal liver hematopoiesis. Cell. 1996;84:321-330.
6. Porcher C, Swat W, Rockwell K, Fujiwara Y, Alt FW, Orkin SH. The T cell leukemia oncoprotein SCL/tal-1 is essential for development of all hematopoietic lineages. Cell. 1996;86:47-57.
7. Tsai FY, Keller G, Kuo FC, et al. An early haematopoietic defect in mice lacking the transcription factor GATA-2. Nature. 1994;371:221-226.
8. Robert-Moreno A, Espinosa L, de la Pompa JL, Bigas A. RBPjkappa-dependent Notch function regulates Gata2 and is essential for the formation of intra-embryonic hematopoietic cells. Development. 2005;132:1117-1126.
9. Kurokawa M, Hirai H. Role of AML1/Runx1 in the pathogenesis of hematological malignancies. Cancer Sci. 2003;94:841-846.
10. Lebestky T, Jung SH, Banerjee U. A Serrate-expressing signaling center controls Drosophila hematopoiesis. Genes Dev. 2003;17:348-353.
11. Burns CE, Traver D, Mayhall E, Shepard JL, Zon LI. Hematopoietic stem cell fate is established by the Notch-Runx pathway. Genes Dev. 2005;19:2331-2342.
12. Mandal L, Banerjee U, Hartenstein V. Evidence for a fruit fly hemangioblast and similarities between lymph-gland hematopoiesis in fruit fly and mammal aorta-gonadal-mesonephros mesoderm. Nat Genet. 2004;36:1019-1023.
13. Conlon RA, Reaume AG, Rossant J. Notch1 is required for the coordinate segmentation of somites. Development. 1995;121:1533-1545.
14. Goyama S, Yamaguchi Y, Imai Y, et al. The transcriptionally active form of AML1 is required for hematopoietic rescue of the AML1-deficient embryonic para-aortic splanchnopleural (P-Sp) region. Blood. 2004;104:3558-3564.
15. Nakano T, Kodama H, Honjo T. Generation of lymphohematopoietic cells from embryonic stem cells in culture. Science. 1994;265:1098-1101.
16. Kitamura T, Koshino Y, Shibata F, et al. Retrovirus-mediated gene transfer and expression cloning: powerful tools in functional genomics. Exp Hematol. 2003;31:1007-1014.
17. Tanaka K, Tanaka T, Kurokawa M, et al. The AML1/ETO(MTG8) and AML1/Evi-1 leukemia-associated chimeric oncoproteins accumulate PEBP2beta(CBFbeta) in the nucleus more efficiently than wild-type AML1. Blood. 1998;91:1688-1699.
18. Imai Y, Kurokawa M, Yamaguchi Y, et al. The corepressor mSin3A regulates phosphorylation-induced activation, intranuclear location, and stability of AML1. Mol Cell Biol. 2004;24:1033-1043.
19. Zhang DE, Hetherington CJ, Meyers S, et al. CCAAT enhancer-binding protein (C/EBP) and AML1 (CBF alpha2) synergistically activate the macrophage colony-stimulating factor receptor promoter. Mol Cell Biol. 1996;16:1231-1240.
20. Durst KL, Hiebert SW. Role of RUNX family members in transcriptional repression and gene silencing. Oncogene. 2004;23:4220-4224.
21. Imai Y, Kurokawa M, Izutsu K, et al. Mutations of the AML1 gene in myelodysplastic syndrome and their functional implications in leukemogenesis. Blood. 2000;96:3154-3160.
22. Kageyama R, Ohtsuka T, Hatakeyama J, Ohsawa R. Roles of bHLH genes in neural stem cell differentiation. Exp Cell Res. 2005;306:343-348.
23. Kunisato A, Chiba S, Nakagami-Yamaguchi E, et al. HES-1 preserves purified hematopoietic stem cells ex vivo and accumulates side population cells in vivo. Blood. 2003;101:1777-1783.
24. Devgan V, Mammucari C, Millar SE, Brisken C, Dotto GP. p21WAF1/Cip1 is a negative transcriptional regulator of Wnt4 expression downstream of Notch1 activation. Genes Dev. 2005;19:1485-1495.
25. Kamakura S, Oishi K, Yoshimatsu T, Nakafuku M, Masuyama N, Gotoh Y. Hes binding to STAT3 mediates crosstalk between Notch and JAK-STAT signalling. Nat Cell Biol. 2004;6:547-554.
26. Stockhausen MT, Sjolund J, Axelson H. Regulation of the Notch target gene Hes-1 by TGFalpha induced Ras/MAPK signaling in human neuroblastoma cells. Exp Cell Res. 2005;310:218-228.
27. McLarren KW, Lo R, Grbavec D, Thirunavukkarasu K, Karsenty G, Stifani S. The mammalian basic helix loop helix protein HES-1 binds to and modulates the transactivating function of the runt-related factor Cbfa1. J Biol Chem. 2000;275:530-538.
28. Zamurovic N, Cappellen D, Rohner D, Susa M. Coordinated activation of notch, Wnt, and transforming growth factor-beta signaling pathways in bone morphogenic protein 2-induced osteogenesis. Notch target gene Hey1 inhibits mineralization and Runx2 transcriptional activity. J Biol Chem. 2004;279:37704-37715.
29. Garg V, Muth AN, Ransom JF, et al. Mutations in NOTCH1 cause aortic valve disease. Nature. 2005;437:270-274.
30. Yoder MC, Hiatt K, Dutt P, Mukherjee P, Bodine DM, Orlic D. Characterization of definitive lymphohematopoietic stem cells in the day 9 murine yolk sac. Immunity. 1997;7:335-344.

GENES, CHROMOSOMES & CANCER 45:482–494 (2006)

Genomewide Screening of DNA Copy Number Changes in Chronic Myelogenous Leukemia with the Use of High-Resolution Array-Based Comparative Genomic Hybridization

Noriko Hosoya,[1,2] Masashi Sanada,[1] Yasuhito Nannya,[1] Kumi Nakazaki,[1] Lili Wang,[1] Akira Hangaishi,[1] Mineo Kurokawa,[1] Shigeru Chiba,[1,2] and Seishi Ogawa[1,3,4]*

[1]Department of Hematology and Oncology, Graduate School of Medicine, University of Tokyo, Tokyo, Japan
[2]Department of Cell Therapy and Transplantation Medicine, University of Tokyo Hospital, University of Tokyo, Tokyo, Japan
[3]Department of Regeneration Medicine for Hematopoiesis, Graduate School of Medicine, University of Tokyo, Tokyo, Japan
[4]Core Research for Evolutional Science and Technology, Japan Science and Technology Corporation, Saitama, Japan

Chronic myelogenous leukemia (CML) evolves from an indolent chronic phase (CP) characterized by the Philadelphia chromosome. Without effective therapy, it progresses to an accelerated phase (AP) and eventually to a fatal blast crisis (BC). To identify the genes involved in stage progression in CML, we performed a genomewide screening of DNA copy number changes in a total of 55 CML patients in different stages with the use of the high-resolution array-based comparative genomic hybridization (array CGH) technique. We constructed Human 1M arrays that contained 3,151 bacterial artificial chromosome (BAC) DNAs, allowing for an average resolution of 1.0 Mb across the entire genome. In addition to common chromosomal abnormalities, array CGH analysis unveiled a number of novel copy number changes. These alterations included losses in 2q26.2–q37.3, 5q23.1–q23.3, 5q31.2–q32, 7p21.3–p11.2, 7q31.1–q31.33, 8pter-p12(p11.2), 9p, and 22q13.1–q13.31 and gains in 3q26.2–q29, 6p22.3, 7p15.2–p14.3, 8p12, 8p21.3, 8p23.2, 8q24.13–q24.21, 9q, 19p13.2–p12, and 22q13.1–q13.32 and occurred at a higher frequency in AP and BC. Minimal copy number changes affecting even a single BAC locus were also identified. Our data suggests that at least a proportion of CML patients carry still-unknown cryptic genomic alterations that could affect a gene or genes of importance in the disease progression of CML. This article contains Supplementary Material available at http://www.interscience.wiley.com/jpages/1045-2257/suppmat.

INTRODUCTION

Chronic myelogenous leukemia (CML) is a clonal disorder originating from pluripotent hematopoietic stem cells that is characterized by the Philadelphia (Ph) chromosome generated by the t(9;22)(q34;q11) (Rowley, 1973; Melo et al., 2003). CML typically shows 3 clinical stages: the initial indolent chronic phase (CP), followed by the intermediate accelerated phase (AP), and then the terminal fatal stage, blast crisis (BC). The prognosis of patients in BC is still very poor, with a median survival of only a few months (Calabretta and Perrotti, 2004). At present, no promising curative therapeutic options are available for patients in BC. The recent development of imatinib mesylate, which selectively inhibits enhanced tyrosine kinase activity of the chimeric BCR–ABL oncoprotein generated by the Ph chromosome, produced impressive therapeutic effects on patients in CP. However, the benefits from this drug seem short-lived once patients progressed to BC (Calabretta and Perrotti, 2004). Thus, to develop new therapeutic approaches for patients in BC, it is essential to identify molecular targets of blastic transformation.

The BC stage of CML is commonly associated with nonrandom secondary chromosomal changes that, in addition to the t(9;22), include +Ph, +8, i(17q), +19, t(3;21)(q26;q22), and t(7;11)(p15;p15) (Prigogina et al., 1978; Alimena et al., 1987; Blick et al., 1987; Melo et al., 2003), or with mutations in

Supported by: Grant-in-Aid for Scientific Research on Priority Areas, Ministry of Education, Culture, Sports, Science and Technology (MEXT); Grant number: KAKENHI 17013022, Grant-in-Aid for Scientific Research, Japan Society for the Promotion of Science (JSPS); Grant number: KAKENHI 16390272, Research on Human Genome, Tissue Engineering, Health and Labour Sciences Research Grants, Ministry of Health, Labour and Welfare; Japan Health Sciences Foundation.

*Correspondence to: Seishi Ogawa, Department of Hematology and Oncology, Department of Regeneration Medicine for Hematopoiesis, Graduate School of Medicine, University of Tokyo, 7-3-1, Hongo, Bunkyo-ku, Tokyo 113-8655, Japan.
E-mail: sogawa-tky@umin.ac.jp

Received 19 October 2005; Accepted 22 November 2005
DOI 10.1002/gcc.20303
Published online 19 January 2006 in Wiley InterScience (www.interscience.wiley.com).